functional regulation of PML and the therapeutic mechanisms of treatment with HDAC inhibitors.

EXPERIMENTAL PROCEDURES

Antibodies, Plasmids, and Cell Culture—The sources of antibodies and plasmids and the cell culture conditions are detailed in the supplemental data.

Transient Transfection, Immunoprecipitation, Immunoblotting, Immunofluorescence, and in Vitro and in Vivo Acetylation Assays—These were performed as described previously (21, 28) except transient transfections into PML$^{-/-}$ MEFs were performed by nucleofection using the Nucleofector system (Amaxa Biosystems) according to the manufacturer's instructions.

Antibody Array Assay and Detection and Quantification of Apoptosis—These are also detailed in the supplemental data.

In Vitro Sumoylation Assay—The *in vitro* sumoylation assay was performed essentially as described previously (21), except recombinant SUMO E1 ligase purchased from BIOMOL International was used instead of HeLa cell lysate.

Cell Sorting—Cell sorting was performed using BD FACSAria Cell Sorter (BD Biosciences) according to the manufacturer's instructions.

RESULTS

PML Exists as an Acetylated Protein in HeLa Cells Treated with Trichostatin A—HDAC inhibitors including TSA induce differentiation, growth arrest, and apoptosis of cancer cells. In addition to their effects on histones, HDAC inhibitors increase the acetylation level of several non-histone proteins, such as transcription factors, cytoskeletal proteins, and molecular chaperones, which are important for their effects on cancer cells (18). These observations prompted us to screen new acetylation targets of TSA with an antibody array assay combined with *in vivo* labeling of acetylated proteins with [^{14}C]acetate. Seven spots indicating possible targets of TSA-induced acetylation were detected (supplemental Fig. S1 and Fig. 1*A*). We focused on one of these targets, PML, a multifunctional protein that is involved in apoptosis, tumor suppression, and cell cycle regulation (2). We set out to confirm whether PML was acetylated *in vivo*. The same anti-PML antibody as used in the antibody array assay immunoprecipitated an ~79-kDa acetylated protein from lysates of TSA-treated HeLa cells (Fig. 1*B*), suggesting that PML existed as an acetylated protein in them. Of note, the antibody we used detected only a single band of PML, although PML has seven isoforms. The antibody was confirmed to be able to detect all PML isoforms, suggesting that this PML was the main one expressed in HeLa cells (supplemental Fig. S1).

PML Is Acetylated by p300 and GCN5 in Vitro—To test whether known histone acetyltransferases (HATs), p300 and GSN5, can acetylate PML, we performed an *in vitro* acetylation assay using GST-PML as a substrate. Both HATs acetylated PML *in vitro* (Fig. 2*A*), and we focused on the acetylation by p300 that occurred with higher efficiency. Use of a series of PML subdomains in the *in vitro* p300 acetylation assay indicated that PML would be acetylated on the C-terminal domain, amino acids 448–560 (supplemental Fig. S2). Inspection of the

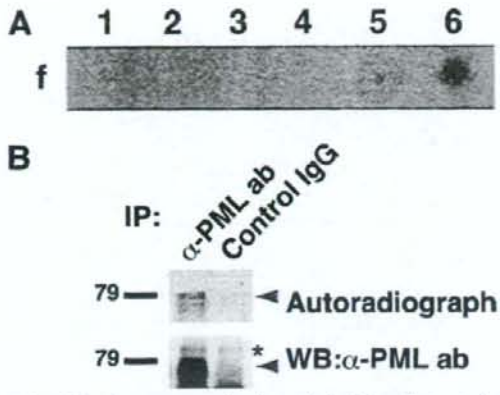

FIGURE 1. **PML exists as an acetylated protein in HeLa cells treated with TSA.** *A*, screening for acetylation targets of TSA by antibody array. Lysate from HeLa cells pulse-labeled with [^{14}C]acetate and treated with TSA was incubated with a nitrocellulose array comprising 113 antibodies. After extensive washes, the array was subjected to autoradiography. Similar results were obtained from duplicated experiments. Representative spots are shown. The antibodies used for *f-1* to *f-6* are anti-MEK1/2 antibody, anti-phospho-MEK1/2 antibody, anti-MKP-1 (V-15) antibody, anti-PML (PG-M) antibody, anti-PML (H-238) antibody, and anti-acetylated lysine antibody, respectively. *B*, PML exists as an acetylated protein in TSA-treated HeLa cells. Pulse-labeled HeLa cells with TSA treatment were lysed as in *A*. The lysates were immunoprecipitated (*IP*) with PML antibody (*ab*) or control rabbit IgG. 90% of the immunoprecipitates were subjected to SDS-PAGE, autoradiography, and detection with phosphorimaging (*upper panel*). 10% of the immunoprecipitates were subjected to SDS-PAGE and immunoblotting with PML antibody (*lower panel*). The positions of PML and nonspecific band are indicated by an *arrow* and an *asterisk*, respectively. *WB*, Western blotting.

PML sequence in this region revealed the presence of 7 lysine residues (supplemental Fig. S2); therefore, we introduced a series of arginine substitutions to map the acetylation sites. Within the C-terminal domain of PML, only the substitution of arginine for lysine 487 (K487R) measurably reduced acetylation of PML by p300 among all the individual substitutions (Fig. 2*B*; mutations are designated by the codon number between Lys and Arg). When arginine substitutions for other lysines were combined with K487R, a further reduction of acetylation was observed with K515R (Fig. 2*C*). Acetylation of full-length PML was impaired by substitutions of K487R and K487R/K515R similarly to that of the C-terminal domain of PML (Fig. 2*D*). Our results indicate that the principal sites of p300 acetylation in PML will be lysines 487 and 515.

PML Acetylation Is Increased in Response to TSA Treatment—We examined whether PML acetylation by p300 occurred *in vivo* at the same sites as identified *in vitro*. Wild-type PML and PML with the K487R/K515R mutations were designated as PML W and PML M, respectively. Coexpression of p300 enhanced PML W acetylation, whereas acetylation PML M was weak in the basal state and showed no significant response to p300 coexpression (Fig. 3*A*, *top panel*). The efficiency of immunoprecipitation was the same for all samples (Fig. 3*A*, *middle panel*), and the increase in acetylation of a 17-kDa protein by coexpression of p300, which suggested the induction of histone acetylation, was equal between transfectants with PML W and PML M (Fig. 3*A*, *bottom panel*). These results suggest that p300 acetylates PML *in vivo* at the same sites as identified *in vitro*.

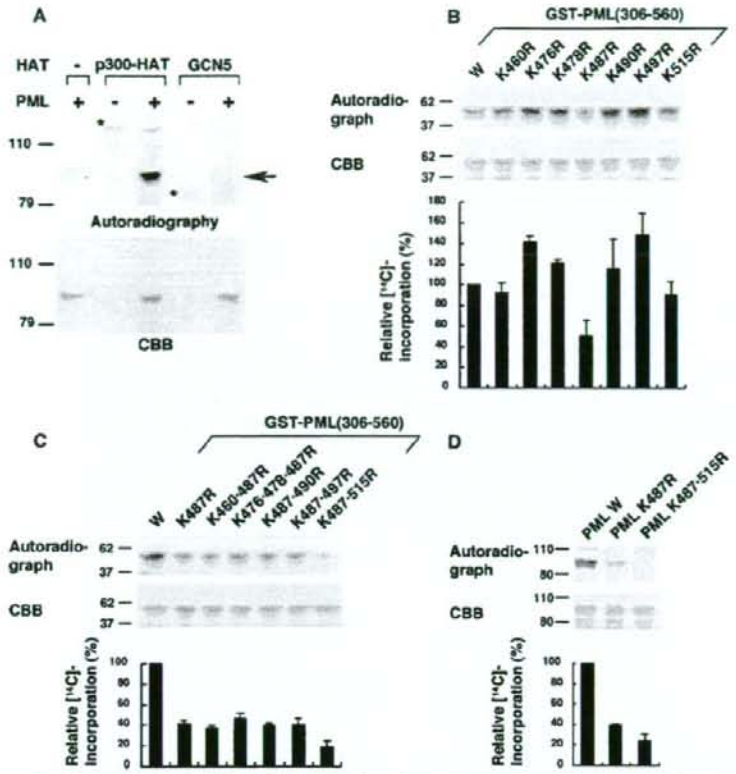

FIGURE 2. **PML acetylation *in vitro*.** *A*, PML is acetylated by p300 and GCN5. GST-PML was incubated with [^{14}C]acetyl-CoA and the indicated HATs. The reaction mixtures were subjected to SDS-PAGE, Coomassie Brilliant Blue (*CBB*) staining, and autoradiography. The positions of acetylated PML and acetylases are indicated by an *arrow* and *asterisks*, respectively. *B* and *C*, identification of PML acetylation sites. Wild-type or mutant GST-PML (amino acids 306–560) were subjected to *in vitro* acetylation by p300-HAT as in *A*. ^{14}C incorporation into each GST-PML construct was quantified using phosphorimaging. A representative phosphorimaging scan (*top panel*), the corresponding CBB-stained electrophoretogram (*middle panel*), and the quantitation of the ^{14}C incorporation for each mutant, relative to the wild-type PML construct (*bottom panel*), are presented. The averages of three independent analyses and standard deviations are shown. *D*, mutation of lysines in full-length PML reduced acetylation by p300. Wild-type or mutant GST-PML (full-length) were subjected to *in vitro* acetylation assays as described in *B*.

Next, we tested whether PML acetylation is induced by TSA. Similarly to the case of p300 coexpression, TSA treatment enhanced PML W acetylation, whereas acetylation of PML M was significantly reduced and showed no significant response to TSA treatment (Fig. 3*B*, *top panel*). Our results suggest that PML is an acetylation target of TSA and that PML acetylation in response to TSA largely occurs at the sites of acetylation by p300.

Acetylation of PML in Response to TSA Is Associated with Enhanced PML Sumoylation—Because one of the PML acetylation sites, lysine 487, is located in the putative nuclear localization signal (amino acids 476–490), we first examined whether PML acetylation affected its nuclear localization to see the effect of acetylation on PML function. However, TSA treatment and the acetylation-defective mutation did not obviously affect PML nuclear localization or accumulation to NBs in immunofluorescent staining (supplemental Fig. S3). We next investigated whether PML acetylation affected its sumoylation, which is required for PML to exercise many of its functions. We set up an *in vivo* sumoylation system in which conjugation of SUMO to PML could be detected by Western analysis, resulting in the appearance of a novel 100-kDa protein expected to be sumoylated PML (21). In this system, coexpression of p300 and exposure to TSA resulted in a significant increase in sumoylation of PML W, whereas sumoylation of PML M was weak and not obviously affected by these treatments (Fig. 4, *A* and *B*). These results suggest the possibility that PML acetylation at lysines 487 and 515 enhances its sumoylation. Next, to verify that acetylated PML is directly sumoylated, we set up an *in vitro* sumoylation system in which recombinant HA-tagged PML protein was incubated with recombinant SUMO E1 and E2 ligase and SUMO with or without a prior acetylation reaction using [^{14}C]acetyl-CoA. Autoradiography visualizing only acetylated PML demonstrated that acetylated PML was efficiently sumoylated (Fig. 4*C*, *upper panel*). Of note, sumoylation efficiency observed in the autoradiograph was much higher than that in immunoblotting with anti-HA antibody where acetylated and nonacetylated PML were visualized (Fig. 4*C*, *upper panel*, *lane 2 versus lower panel*, *lane 2*). These results indicate that acetylated PML may be preferentially sumoylated *in vitro*.

PML Acetylation May Play an Important Role in TSA-induced Apoptosis—TSA treatment induces apoptosis in HeLa cells by unknown mechanisms (16). In our previous study, PML sumoylation plays an important role in As_2O_3-induced apoptosis (21). Given our findings that PML acetylation is associated with increased PML sumoylation, this may represent one of the mechanisms of TSA-induced apoptosis. We first examined whether PML was involved in TSA-induced apoptosis. For this purpose, we established HeLa cells stably transfected with an expression vector for small hairpin RNA against PML and an empty control vector and designated them as PML KD HeLa and control KD HeLa, respectively. Successful knocking down of PML was confirmed by immunofluorescence analysis with an anti-PML antibody (supplemental Fig. S4). TSA treatment caused the appearance of a sub-G_1 peak in cell cycle analysis, a marker of apoptosis, in both cells. However, the ratio of apoptotic cells was reduced by ~60% in PML KD HeLa compared with control KD HeLa, suggesting the involvement of PML in

TSA-induced apoptosis (Fig. 5*A* and supplemental Fig. S5). We examined further using PML$^{-/-}$ MEFs. Notably, overexpression of PML W in PML$^{-/-}$ MEFs substantially increased TSA-induced apoptosis relative to cells transfected with an empty vector, whereas, PML M displayed an impaired ability to mediate apoptosis in response to TSA (Fig. 5*B* and supplemental Fig. S6). An equal expression level of PML between PML W and PML M transfectants was confirmed (supplemental Fig. S6). These results further support the involvement of PML in TSA-induced apoptosis and suggest the importance of PML acetylation in conferring apoptosis by TSA.

Next, we investigated the effect of PML sumoylation on PML-mediated apoptosis in response to TSA. Cotransfection of expression vectors for SUMO and Ubc9 further sensitized PML W transfectants to TSA-induced apoptosis (Fig. 5*C*, *third* and *fourth lanes*), whereas the proapoptotic effects of SUMO and Ubc9 were greatly reduced in control and PML M transfectants (Fig. 5*C*, *first* and *second lanes* and *fifth* and *sixth lanes*). Enhanced sumoylation of PML W induced by TSA and impaired sumoylation of PML M were observed also in PML$^{-/-}$ MEFs (Fig. 5*D*). These results suggest that sumoylation enhances PML-mediated apoptosis in response to TSA. To test this hypothesis, we created an expression vector for the PML-3K mutant, which had lysine-to-arginine mutations at all three PML sumoylation sites and cannot be sumoylated (22). Overexpression of PML-3K in either the presence or absence of SUMO and Ubc9 had little or no effect on TSA-induced apoptosis (Fig. 5*C*, *seventh* and *eighth lanes*), indicative of a requirement for PML sumoylation in TSA-mediated apoptosis. These results suggest the hypothesis that enhanced PML sumoylation through PML acetylation is one of the mechanisms of TSA-induced apoptosis.

Finally, to investigate the generality of the effects of TSA on PML among HDAC inhibitors, we used depsipeptide, another HDAC inhibitor that belongs to a different class. Depsipeptide enhanced acetylation and sumoylation of PML, and its apoptotic effect was increased by PML expression similarly to TSA (supplemental Fig. S8). These results further support the hypothetical importance of PML acetylation in HDAC inhibitor-induced apoptosis.

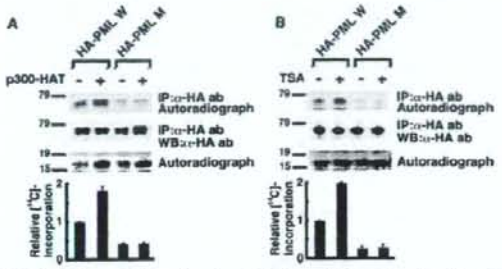

FIGURE 3. **PML acetylation *in vivo*.** *A*, PML acetylation is induced by p300 cotransfection *in vivo*. HeLa cells were transfected with indicated expression vectors. PML acetylation was analyzed as in Fig. 1*B* except for the use of anti-HA antibody (*ab*) instead of anti-PML antibody for IP and IB. The lysates were also subjected to SDS-PAGE followed by autoradiography to confirm successful induction of histone acetylation by p300-HAT cotransfection. A representative autoradiograph of PML (*top panel*), the corresponding image of IB with anti-HA antibody (*second panel from the top*), and the autoradiograph of histone (*third panel from the top*) are presented. ^{14}C incorporation into PML and the amount of immunoprecipitated (*IP*) PML protein were quantified using analyzer of each imaging system. Relative ^{14}C incorporation adjusted by the efficiency of immunoprecipitation was calculated. The average and standard deviations for two independent analyses are presented (*bottom panel*). *B*, PML acetylation is increased in response to TSA treatment. HeLa cells were transfected with indicated expression vectors and treated with or without 10 μM TSA for 4 h. PML acetylation was analyzed and presented as in *A*. *WB*, Western blotting.

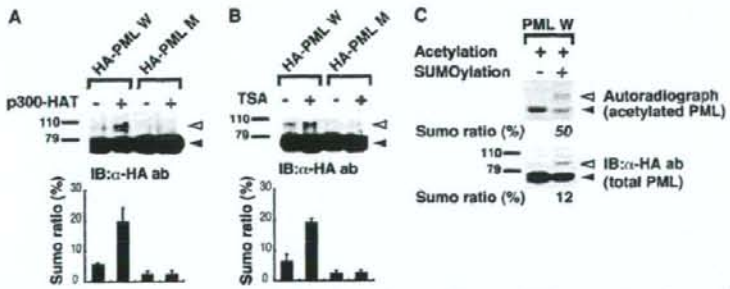

FIGURE 4. **PML acetylation is associated with enhanced sumoylation.** *A*, p300 coexpression enhances PML sumoylation. HeLa cells were transfected with the indicated expression vectors with cotransfection of those for SUMO and Ubc9. The cell lysates were subjected to SDS-PAGE followed by immunoblotting (*IB*) with anti-HA antibody (*ab*). The positions of sumoylated PML detected as an upper shifted band and nonsumoylated PML are indicated by *white* and *black arrowheads*, respectively. The ratios of sumoylated PML to total (sumoylated and unsumoylated PML) were calculated (SUMO ratio) and presented as bar charts. *B*, PML sumoylation increases in response to TSA treatment. PML sumoylation was examined as in *A* except that cells were treated with 10 μM TSA for 4 h instead of cotransfection of p300-HAT. *C*, acetylated PML is preferentially sumoylated *in vitro*. HA-tagged PML protein synthesized *in vitro* was immunoprecipitated with anti-HA antibody and incubated with p300-HAT and [^{14}C]acetyl-CoA as in Fig. 2*A*. The protein was subjected to an *in vitro* sumoylation assay and SDS-PAGE and transferred to a polyvinylidene difluoride membrane. Sumoylation of total (acetylated and nonacetylated) PML was visualized by IB with anti-HA antibody (*lower panel*). The same membrane was also subjected to an autoradiography to visualize sumoylation of acetylated PML (*upper panel*). Sumoylated and nonsumoylated PML are indicated as in *A*. SUMO ratio in each panel were calculated and presented at the *bottom*.

DISCUSSION

The data presented here demonstrate that acetylation of PML may enhance its sumoylation and play an important role in the control of PML-dependent apoptosis in response to TSA exposure. Sumoylation of PML is necessary for NB formation (5, 10), and the apoptotic effects of PML may be dependent on NB formation (see Introduction). Given our findings that PML acetylation is associated with increased PML sumoylation, this sumoylation-dependent NB formation may represent one of the mechanisms by which PML acetylation can enhance apoptosis. This hypothesis is supported by our findings that coexpression of SUMO and Ubc9 enhances PML-dependent apoptosis by TSA, that acetylation-defective mutants of PML exhibit defects in sumoylation and apoptosis in response to TSA treatment, and that a sumoylation-impaired PML mutant (PML-3K) is

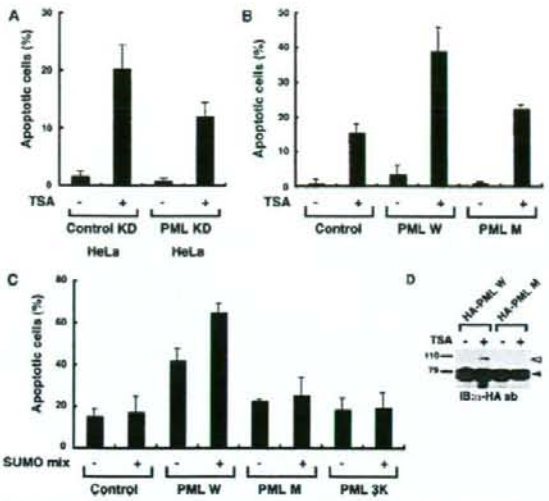

FIGURE 5. **PML acetylation is important for apoptosis induced by TSA.** *A*, PML knockdown reduces TSA-induced apoptosis in HeLa cells. HeLa cells whose PML was stably knocked down (PML KD HeLa) or control cells (Control KD HeLa) were treated with or without 1 μM TSA for 36 h. Apoptotic cells were detected and quantified as described under "Experimental Procedures." The ratios of apoptotic cells are plotted on bar charts. The averages of two independent analyses and standard deviations are shown. *B*, an acetylation-defective mutant of PML displayed impaired ability to mediate TSA-induced apoptosis. $PML^{-/-}$ MEFs were transfected with a bicistronic expression vector for GFP alone (control) or GFP and the indicated PML. GFP^{+} cells were sorted and treated with or without 1 μM TSA for 48 h. Apoptotic cells were analyzed as in *A*. *C*, coexpression of Ubc9 and SUMO enhances PML-mediated apoptosis in response to TSA. The analyses of apoptosis were performed as in *B* except that cells were cotransfected with expression vectors for SUMO and Ubc9 (SUMO mix) or an empty vector as indicated. *D*, increased PML sumoylation induced by TSA in $PML^{-/-}$ MEFs. PML sumoylation in $PML^{-/-}$ MEFs was examined as in Fig. 4*B*. *IB*, immunoblotting; *ab*, antibody.

also defective in TSA-mediated apoptosis. It should be noted that $PML^{-/-}$ MEF cells are still sensitive to apoptosis by TSA, although at a much reduced level compared with cells expressing PML. There may also be PML-independent apoptotic mechanisms that respond to TSA. This is not surprising, considering that TSA alters the expressions of various genes by the acetylation of histones and many kinds of transcription factors such as p53 (see Introduction). More work will be required to determine the individual contributions of these different actions of TSA on the proliferation, survival, and differentiation of cells.

Acetylation of lysine leads to loss of its positive charge. In some cases, arginine, a positive charged amino acid, and glutamine, a noncharged one, are reported to mimic nonacetylated and acetylated lysine, respectively. We examined whether glutamine substitution at acetylation sites, lysines 487 and 515, had an enhancing effect on PML sumoylation. The PML mutant with glutamine substitution, however, showed impaired sumoylation in HeLa cells similarly to the one with arginine substitution (data not shown). Effects of acetylation other than the loss of positive charge or subtle differences of amino acid structure between lysine and glutamine may be important for PML sumoylation.

Recent studies reveal that increasing numbers of proteins are targeted by both acetylation and sumoylation. However, the correlation between these modifications has hardly been investigated except the cases where both modifications competitively target the same lysine residue such as the cases of HIC1 (hypermethylated in cancer 1) and MEF2 (myocyte enhancer factor 2) (23, 24). This is the first report that suggests acetylation-dependent enhancement of sumoylation. Phosphorylation has been reported to regulate sumoylation. Recently, the classical sumoylation consensus motif (ψKXE) with an adjacent proline-directed phosphorylation motif (SP), $\psi KXEXXSP$ motif where ψ is a large hydrophobic residue and X is any residue, has been proposed as a phosphorylation-dependent sumoylation motif (25, 26). Between the two acetylation sites, lysines 487 and 515, lysine 487 is the major acetylation site, and K487R affects sumoylation more than K515R (Fig. 2, *B* and *C*, and data not shown). PML sumoylation is reported to occur at three lysine residues, lysine 65, 160, and 490 (22). It would be interesting to discover whether acetylation at lysine 487 specifically affects sumoylation at any of these lysine residues, especially at the adjacent lysine 490. p53 also has a similar sequence where an acetylated lysine lies adjacent to a sumoylated lysine (supplemental Fig. S9), although the correlation between acetylation and sumoylation has not been investigated (27). $K\psi\psi KXE$ might be a motif of acetylation-dependent sumoylation.

In summary, our studies provide evidence for a new post-transcriptional modification of PML and a new mechanism of regulation of PML sumoylation, and establish a novel relationship between PML and TSA-induced apoptosis. This work provides new insights into the regulation of PML function and the control of protein sumoylation. Considering the large number of binding partners of PML and the key contributions of PML to the stability and function of the NBs, PML acetylation is likely to modulate multiple cell activities beyond apoptosis through regulation of recruitment or release of NBs components.

Acknowledgments—We are very grateful to Ryouhei Tanizaki, Yuka Nomura, and Chika Wakamatsu for technical assistance.

REFERENCES

1. Mu, Z. M., Chin, K. V., Liu, J. H., Lozano, G., and Chang, K. S. (1994) *Mol. Cell. Biol.* **14,** 6858–6867
2. Salomoni, P., and Pandolfi, P. P. (2002) *Cell* **108,** 165–170
3. Wang, Z. G., Delva, L., Gaboli, M., Rivi, R., Giorgio, M., Cordon-Cardo, C., Grosveld, F., and Pandolfi, P. P. (1998) *Science* **279,** 1547–1551
4. Wang, Z. G., Ruggero, D., Ronchetti, S., Zhong, S., Gaboli, M., Rivi, R., and Pandolfi, P. P. (1998) *Nat. Genet.* **20,** 266–272
5. Ishov, A. M., Sotnikov, A. G., Negorev, D., Vladimirova, O. V., Neff, N., Kamitani, T., Yeh, E. T., Strauss, J. F., III, and Maul, G. G. (1999) *J. Cell Biol.* **147,** 221–234
6. Dellaire, G., and Bazett-Jones, D. P. (2004) *Bioessays* **26,** 963–977
7. Dyck, J. A., Maul, G. G., Miller, W. H., Jr., Chen, J. D., Kakizuka, A., and Evans, R. M. (1994) *Cell* **76,** 333–343
8. Koken, M. H., Puvion-Dutilleul, F., Guillemin, M. C., Viron, A., Linares-Cruz, G., Stuurman, N., de Jong, L., Szostecki, C., Calvo, F., Chomienne, C., Degos, L., Puvion, E., and de Thé, H. (1994) *EMBO J.* **13,** 1073–1083
9. Weis, K., Rambaud, S., Lavau, C., Jansen, J., Carvalho, T., Carmo-Fonseca, M., Lamond, A., and Dejean, A. (1994) *Cell* **76,** 345–356
10. Zhong, S., Muller, S., Ronchetti, S., Freemont, P. S., Dejean, A., and Pandolfi, P. P. (2000) *Blood* **95,** 2748–2752

11. Kim, K. I., Baek, S. H., and Chung, C. H. (2002) *J. Cell. Physiol.* **191,** 257–268
12. Muller, S., Matunis, M. J., and Dejean, A. (1998) *EMBO J.* **17,** 61–70
13. Zhu, J., Koken, M. H., Quignon, F., Chelbi-Alix, M. K., Degos, L., Wang, Z. Y., Chen, Z., and de The, H. (1997) *Proc. Natl. Acad. Sci. U. S. A.* **94,** 3978–3983
14. Chen, G. Q., Shi, X. G., Tang, W., Xiong, S. M., Zhu, J., Cai, X., Han, Z. G., Ni, J. H., Shi, G. Y., Jia, P. M., Liu, M. M., He, K. L., Niu, C., Ma, J., Zhang, P., Zhang, T. D., Paul, P., Naoe, T., Kitamura, K., Miller, W., Waxman, S., Wang, Z. Y., de The, H., Chen, S. J., and Chen, Z. (1997) *Blood* **89,** 3345–3353
15. Niu, C., Yan, H., Yu, T., Sun, H. P., Liu, J. X., Li, X. S., Wu, W., Zhang, F. Q., Chen, Y., Zhou, L., Li, J. M., Zeng, X. Y., Yang, R. R., Yuan, M. M., Ren, M. Y., Gu, F. Y., Cao, Q., Gu, B. W., Su, X. Y., Chen, G. Q., Xiong, S. M., Zhang, T., Waxman, S., Wang, Z. Y., Chen, S. J., Hu, J., Shen, Z. X., and Chen, S. J. (1999) *Blood* **94,** 3315–3324
16. Marks, P. A., Richon, V. M., and Rifkind, R. A. (2000) *J. Natl. Cancer Inst.* **92,** 1210–1216
17. Wolffe, A. P., and Pruss, D. (1996) *Cell* **84,** 817–819
18. Glozak, M. A., Sengupta, N., Zhang, X., and Seto, E. (2005) *Gene (Amst.)* **363,** 15–23
19. Bandyopadhyay, D., Mishra, A., and Medrano, E. E. (2004) *Cancer Res.* **64,** 7706–7710
20. Terui, T., Murakami, K., Takimoto, R., Takahashi, M., Takada, K., Murakami, T., Minami, S., Matsunaga, T., Takayama, T., Kato, J., and Niitsu, Y. (2003) *Cancer Res.* **63,** 8948–8954
21. Hayakawa, F., and Privalsky, M. L. (2004) *Cancer Cell* **5,** 389–401
22. Kamitani, T., Kito, K., Nguyen, H. P., Wada, H., Fukuda-Kamitani, T., and Yeh, E. T. (1998) *J. Biol. Chem.* **273,** 26675–26682
23. Stankovic-Valentin, N., Deltour, S., Seeler, J., Pinte, S., Vergoten, G., Guerardel, C., Dejean, A., and Leprince, D. (2007) *Mol. Cell. Biol.* **27,** 2661–2675
24. Gregoire, S., and Yang, X. J. (2005) *Mol. Cell. Biol.* **25,** 2273–2287
25. Hietakangas, V., Anckar, J., Blomster, H. A., Fujimoto, M., Palvimo, J. J., Nakai, A., and Sistonen, L. (2006) *Proc. Natl. Acad. Sci. U. S. A.* **103,** 45–50
26. Yang, X. J., and Gregoire, S. (2006) *Mol. Cell* **23,** 779–786
27. Kwek, S. S., Derry, J., Tyner, A. L., Shen, Z., and Gudkov, A. V. (2001) *Oncogene* **20,** 2587–2599
28. Hayakawa, F., Towatari, M., Ozawa, Y., Tomita, A., Privalsky, M. L., and Saito, H. (2004) *J. Leukocyte Biol.* **75,** 529–540

Leukemia & Lymphoma, December 2008; 49(12): 2359–2364

informa
healthcare

ORIGINAL ARTICLE: RESEARCH

Abnormal cytoplasmic dyslocalisation and/or reduction of nucleophosmin protein level rarely occurs in myelodysplastic syndromes

YUICHI ISHIKAWA[1]*, JINGLAN XU[1]*, GYOSUKE SAKASHITA[2], TAKESHI URANO[2], TATSUYA SUZUKI[1], AKIHIRO TOMITA[1], HITOSHI KIYOI[3], SHIGEO NAKAMURA[4], & TOMOKI NAOE[1]

[1]*Department of Hematology and Oncology, Nagoya University Graduate School of Medicine, Showa-ku, Nagoya, Japan,* [2]*Department of Biochemistry, Shimane University School of Medicine, Izumo, Japan,* [3]*Department of Infectious Diseases, Nagoya University Hospital, Showa-ku, Nagoya, Japan, and* [4]*Department of Pathophysiology, Nagoya University Hospital, Showa-ku, Nagoya, Japan*

(Received 6 September 2008; accepted 8 October 2008)

Abstract
The Nucleophosmin1 (*NPM1*) gene located in chromosome 5q35 is affected by chromosomal translocation, mutation and deletion in myelodysplastic syndrome (MDS) and acute myeloid leukemia (AML). *NPM1* haploinsufficiency reportedly causes MDS-like disorders in knockout mice. Here, we studied mRNA and protein expression in bone marrow (BM) samples from 36 patients with MDS. The *NPM1* expression levels of mRNA and protein were not related to chromosome 5 abnormalities and were almost the same as those in normal BM and AML cells. However, the protein levels in AML cells with *NPM1* mutations were slightly lower than in those without mutation. Immunochemical studies showed no difference in the staining intensity and subcellular localisation between MDS and normal BM cells. It was concluded that abnormal cytoplasmic localisation and/or significant reduction of NPM1 protein level rarely occurs in MDS. The increase in the number of nuclear NPM1-positive cells may be related to the progression of MDS.

Keywords: *Nucleophosmin, myelodysplastic syndrome, immunohistochemical staining*

Introduction

Nucleophosmin1 (NPM1) is a nucleolar phosphoprotein with multiple biological roles [1–5]. In hematological malignancies, the *NPM1* is affected by chromosomal translocation, mutation and deletion [6–8]. The *NPM1* on 5q35 is translocated with the *ALK* in anaplastic large cell lymphoma with t(2;5) [9]. The *MLF1* and *RARA* genes are fused with *NPM1* in myelodysplastic syndrome (MDS)/acute myeloid leukemia (AML) with t(3;5) [10] and acute promyelocytic leukemia with t(5;17) [11], respectively. Most importantly, mutations in exon 12 have been found in a significant proportion of *de novo* AML cases, especially in those with a normal karyotype [12–16]. Mutant NPM is aberrantly localised in the cytoplasm, but the molecular mechanisms associated with leukemia remain unclear. The knockout mice model of the *NPM1* gene suggests that $NPM1^{+/-}$ haploinsufficiency causes hematological disorders like MDS [17]. Because the *NPM1* gene locus on 5q35 is often deleted in MDS and AML, loss-of-heterozygosity and/or mutation have been studied in human MDS samples [18]. According to previous reports, however, mutation of the *NPM1* exon 12 is very rare in MDS either in combination with 5q abnormality or not. Furthermore, the promoter region of *NPM1* is rarely methylated [19], suggesting that *NPM1* may not simply have a role as a tumor suppressor gene in MDS. To further clarify the involvement of *NPM1* in MDS, we generated a new antibody to NPM and

Correspondence: Yuichi Ishikawa, Department of Hematology and Oncology, Nagoya University Graduate School of Medicine, 65 Tsurumai-cho, Showa-ku, Nagoya 466-8560, Japan. Tel: +81-52-744-2955. Fax: +81-52-744-2801. E-mail: yishikaw@med.nagoya-u.ac.jp
*These authors equally contributed to this work.

ISSN 1042-8194 print/ISSN 1029-2403 online
DOI: 10.1080/10428190802541815

analysed the expression levels and subcellular localisation of NPM in MDS.

Materials and methods

Patient samples

NPM1 expression and mutation were analysed in bone marrow (BM) cells and specimens from 36 patients with newly diagnosed MDS at the Nagoya University Hospital. Diagnosis was made according to the FAB classification. MDS patients consisted of 24 men and 12 women with a median age of 58 years (range, 28–89 years). Four secondary AML patients with MDS were also studied. BM mononuclear cells were harvested by standard Ficoll/Paque density gradient centrifugation (Amersham Pharmacia Biosciences, Roozendaal, The Netherlands) and were suspended in RPMI1640 medium supplemented with 10% fetal bovine serum, 100 IU/mL of penicillin G and 100 μg/mL of streptomycin. Informed consent was obtained from all patients to use their samples for banking and molecular analysis, and approval was obtained from the ethical committee of Nagoya University School of Medicine for these studies.

Antibodies

Anti-NPM mouse monoclonal antibody (NPM9.2.6) specific for bacterially expressed NPM1 was generated, then, purified from BL21 transformed with pGEX 4T-2 carrying full-length human NPM1. To determine the epitope of this antibody, HeLa cells were transfected for 48 h with human NPM1, NPM1.2 and their truncated mutants were tagged with EGFP. Cells were then lysed with SDS-sample buffer followed by sonication. Western blot analysis was performed with anti-NPM 9.2.6 and anti-EGFP rabbit polyclonal antibody (MBL). To characterise the cross-reactivity between species, lysates were prepared from HeLa and NIH3T3 cells. Western blot analysis was performed with anti-NPM 9.2.6, anti-B23 mouse monoclonal antibody (B0556, Sigma) and anti-αtubulin mouse monoclonal antibody (T6199, Sigma).

Characterisation of anti NPM 9.2.6 monoclonal antibody

Anti-NPM mouse monoclonal antibody 9.2.6 can recognise both human NPM1 and NPM1.2, the epitope of which is located in the region of 170–189 aa (Supplement Figure 1A). However, this antibody cannot recognise mouse NPM (Supplement Figure 1B, upper panel) despite the expression level being comparable between the cell lines (Supplement Figure 1B, middle panel).

Real time quantitative PCR

Total RNA was extracted from the samples by using a QIAamp RNA Blood Mini Kit (Qiagen, Chatsworth, CA). cDNA was synthesised from each RNA using a random primer and Moloney murine leukemia virus reverse transcriptase (SuperScript II; Invitrogen) according to the manufacturer's recommendations. The expression level of NPM1 transcripts were quantified using a real-time fluorescence detection method on an ABI prism7000 sequence detection system following the manufacturer's recommendations (Applied Biosystem, Foster City, CA). PCR procedures were carried out at 50°C for 2 min, 95°C for 10 min, followed by 40 PCR cycles at 95°C for 15 s and 60°C for 1 min. The housekeeping gene, GAPDH, served as a control for cDNA quality. Each gene expression level was analysed in duplicate and the expression level was calculated as previously described [20].

Screening for mutation of the NPM1 gene

For the screening of *NPM1* mutations, we amplified genomic DNA corresponding to exon 12 of *NPM1* by PCR using the primers NPM1-F, 5′-TTAACTCTCTGGTGGTAGAATGAA-3′ and NPM1-R, 5′-CAAGACTATTTGCCATTCC TAAC-3′, as previously reported [6]. Amplified products were separated through agarose gel, purified using a QIAquick gel extraction kit (Qiagen) and directly sequenced on a DNA sequencer (310; Applied Biosystems) using a BigDye terminator cycle sequencing kit (Applied Biosystems). If mutations were found by direct sequencing, the fragments were cloned into a pGEM-T Easy vector (Promega, Madison, WI), then transfected into *Escherichia coli* strain DH5α. At least four recombinant colonies were selected and plasmid DNA was prepared using a QIAprep Spin Miniprep Kit (Qiagen) and sequenced.

Immunohistochemical staining

Samples were fixed with ice-cold 4% paraformaldehyde for 16–24 h, embedded in paraffin, sectioned transversely (thickness, 3 μm) and processed so that immunohistochemical techniques could be used to determine the localisation of NPM. After removal of paraffin with xylene and dehydration with a series of ethanol solutions, the tissue sections were subjected to microwave irradiation (750 W) for 15 min in 0.01 mol/L citrate buffer (pH 6.0). The sections were then placed in

an automated immunostainer (Ventana Medical Systems, Tucson, AZ) as described [21]. For negative controls, primary antibodies were replaced with mouse IgG. We investigated a single case twice for NPM expression. The entire section was screened to find the region with the highest immunostaining.

Immunoblotting

A total of $1-5\times10^6$ fresh or frozen cells were directly lysed in sample buffer and then subjected to SDS-polyacrylamide gel electrophoresis on a 10% gel and the separated proteins were then transferred to a polyvinylidene difluoride membrane (Millipore Corp., Bedford, MA, USA). The membrane was incubated at room temperature first for 1 h with 5% non-fat milk and 0.1% Tween-20 in Tris-buffered saline and then kept overnight with the appropriately diluted mouse monoclonal antibodies in the same solution. After washing, the membrane was incubated for 1 h with diluted horseradish peroxidase-conjugated mouse antibody to mouse IgG (MBL) and immune complexes were then detected with ECL reagents (Amersham).

Results

The expression level of the *NPM1* transcripts in MDS cells was studied and compared with those in normal and AML cells (Figure 1). In normal peripheral blood, the median expression level of the *NPM1* transcripts was 8.0 (range, 3.2–9.5) $\times 10^6$, 9.4 (range, 1.6–12) $\times 10^6$, 10.8 (7.2–22) $\times 10^6$ copies/μg RNA in normal peripheral blood cells, cord blood cells and BM cells, respectively. The median expression levels in MDS cells was 2.0 (range, 0.2–83) $\times 10^6$ copies/μg RNA, which was a lower level than that those of normal cells, but the expression levels of *NPM1* transcripts were not statistically different between MDS samples and normal BM samples ($p=0.163$, by Mann–Whitney test). In two patients with secondary AML carrying a 5q abnormality, the mRNA level was not lower. Mutations in exon 12 of the NPM1 gene were analysed in 36 patients with RA, RAEB and RAEB-T. In two (5%) patients with RAEB, 4-bp was inserted into the common site of exon 12, and mRNA levels in both cases were the same as for those without the mutation.

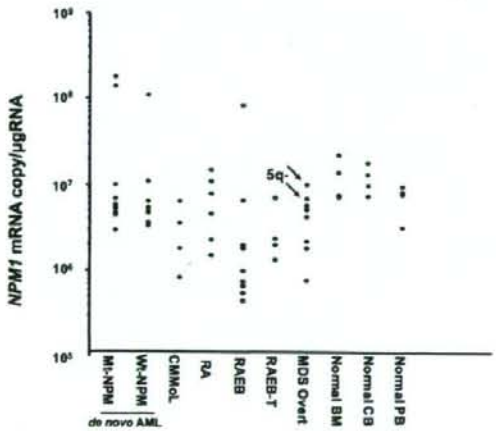

Figure 1. Real-time quantitative PCR of NPM1 transcripts. Distribution of the expression level of the NPM1 mRNA in AML, MDS and normal samples are indicated, the arrowed dots indicate that the patients carrying a 5q- abnormality. There were no significant differences in the sequence of exon12 of *NPM1*, the FAB type and normal samples.

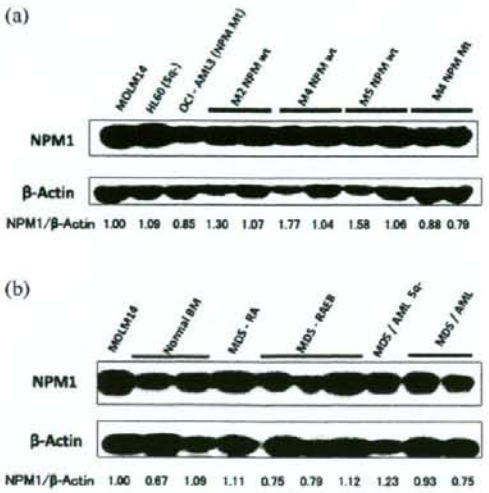

Figure 2. NPM1 protein detected by immunoblotting. The expression level of NPM1 protein in clinical samples and cell lines was analysed by immunoblotting. Protein signal intensities were measured and normalised with the signal intensities of β-actin. The normalised NPM1 β-actin ratio is indicated below, the ratio of MOLM14 cell is used as a control. (A) In AML cell line, the expression level of NPM1 in HL60 cell carrrying 5q deletion was almost equally to that of MOLM14 cell carrying intact chromosome 5, each cell lines possesed wild-type NPM1. Although in OCI-AML3 cell carrying *NPM1* mutation, the slightly lower expression of NPM1 protein level was observed. In AML samples, immunoblotting analysis of M2, M4 with and M5 according to FAB classification samples with wild-type *NPM1* revealed that the expression level of NPM1 protein was almost at the same level as the FAB type. In AML samples with mutated *NPM1*, the expression level of NPM1 protein was slightly lower than that in AML cells without *NPM1* mutation, in spite of the same FAB type. (B) The expression level of NPM1 protein was compared in MDS samples according to FAB type and normal bone marrow mononuclear cells. There was no significance in the difference in expression level of NPM1 protein between MDS samples with or without 5q- and normal BM samples.

To study the levels of NPM1 protein expression, a total of 21 samples from healthy volunteers, AML patients and MDS patients were subjected to immunoblot analysis. Anti-NPM antibody (9.2.6) detected bands at a molecular weight of 37 kDa, corresponding to NPM, in all samples. The NPM level in AML cells with *NPM1* mutation was slightly lower than that in AML cells without *NPM1*

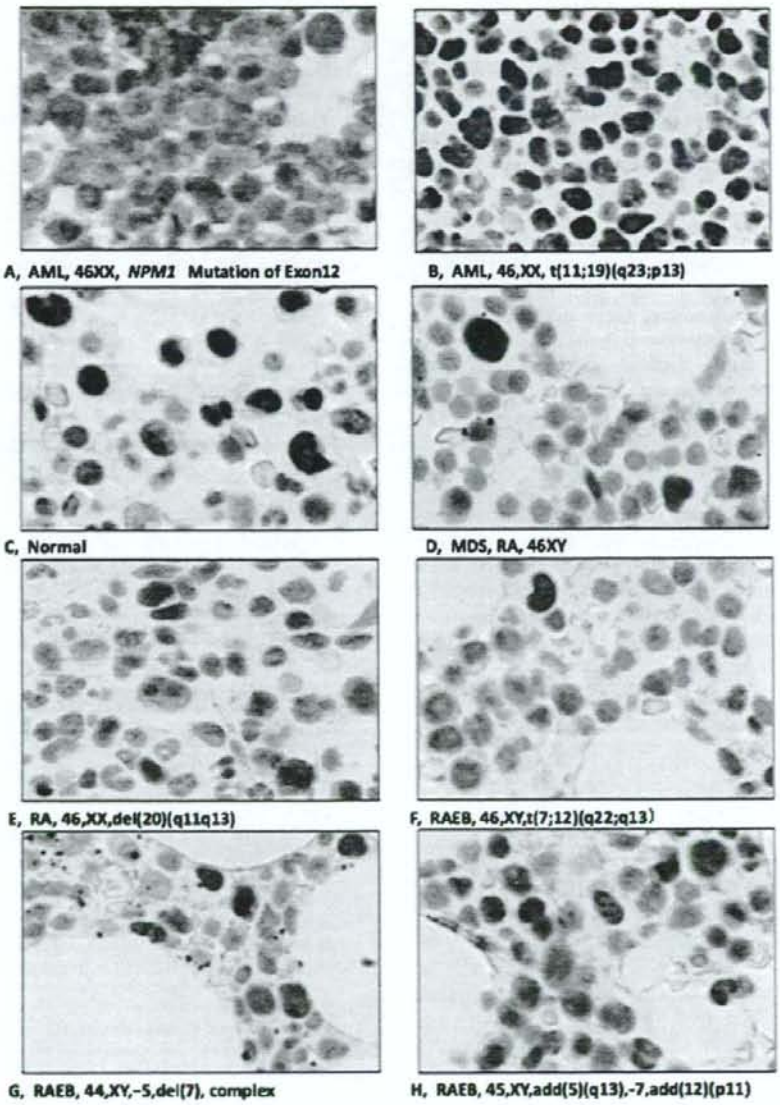

Figure 3. Immunohistochemistry of NPM1. The immunohistochemical studies of the NPM1 in AML, MDS and normal samples are indicated with karyotype. (A) In AML with *NPM1* mutation, NPM was diffusely stained in a microgranular pattern in the cytoplasm as well as the nucleus, as reported previously. (B) In AML without *NPM1* mutation, nuclear and nucleolar staining was clearly detected in leukemia cells. (C) In Normal BM cells, nuclear and nucleolar staining was detected in a part of lymphoid and myeloid cells. (D–H) In MDS, positive nuclear staining was observed in relatively large myeloid cells, which was similar to the staining pattern in normal BM.

mutation (mean relative intensity: 0.85 *vs.* 1.08, $p = 0.01$, Figure 2A). In MDS, the expression levels varied among samples but the expression level was similar to that of AML cells without *NPM1* mutation (0.93 *vs.* 1.08, $p = 0.13$, Figure 2A). No aberrant bands were detected in these samples (Figure 2B).

Using newly generated anti-NPM monoclonal antibody (NPM 9.2.6), both NPM1.1 and NPM1.2 proteins were detected by immunoblot analysis and immunohistochemical techniques. In normal BM cells, NPM1 was clearly detected in mononuclear myeloid cells but not in polymorphonuclear cells and erythroblasts. Lack of NPM1 expression in the polymorphonuclear cells was confirmed using normal peripheral blood by immunoblot analysis and immunohistochemical techniques (Supplement Figure 2). In AML specimens with *NPM1* mutation (Figure 3A) as a control, diffusely stained NPM1 could be observed as a microgranular pattern in the cytoplasm as well as the nucleus, as reported previously. In AML specimens without *NPM1* mutation (Figure 3B) as another control, nuclear and nucleolar staining was clearly detected in leukemia cells.

In MDS specimens (Figure 3D–H), positive nuclear staining was observed in relatively large myeloid cells, which was fundamentally similar to the staining pattern in normal BM (Figure 3C). However, the percentage of NPM-positive cells in the specimen was significantly decreased, which is explained by the percentage of mature cells such as polymorphonuclear cells and lymphocytes, as well as erythroblasts. There are no specimens in which NPM showed subcellular localisation which was different from normal BM cells.

Discussion

MDS is a clonal hematopoietic stem cell disorder characterised by multi-lineage dysplasia and pancytopenia in which the molecular mechanism is still mainly unclear, and even that which is understood is, quite heterogeneous [22]. Recently, it was suggested that *NPM1* might play the role of a tumor-suppressor gene in MDS in light of findings that $NPM1^{+/-}$ heterozygous mice develop a hematologic syndrome with features of human MDS [17]. During a long-time observation, $NPM1^{+/-}$ mice developed lymphoid malignancies and solid tumors, in addition to myeloid malignancies [23]. Malignant cells displayed multiple centrosomes and retained the wild-type allele and NPM1 protein with normal subcellular localisation and expression level. If this haploinsufficiency model is applicable to human MDS, the expression level of NPM1 must be critical for development or suppression of MDS. According to Knudson's two-hit model, two successive events, such as a deletion, mutation or methylation, in both alleles of a tumor-suppressor gene are required to turn a normal cell into a cancer cell [23]. In this case, the tumor-suppressor protein almost loses its function entirely. Because NPM1 has a critical role in ribosome biogenesis and cell proliferation, a haploinsufficiency model rather than Knudson's two-hit model may fit better with the above mice model. So far no study has carefully investigated the expression of NPM1 in human MDS samples. Here, we indicated that NPM1 protein levels were not significantly decreased in MDS cells irrespective of the presence of a 5q abnormality. Although accurate quantification of protein expression is difficult in clinical samples, our study showed that NPM1 levels in AML cells with *NPM1* mutation were lower than that in AML cells without *NPM1* mutation. Mutated NPM protein might have a shorter half-life than wild-type NPM as well as being localised in the cytoplasm. But, it is needed to study more samples to elucidate the differences of NPM protein levels in AML cells with or without *NPM1* mutation.

The immunohistochemical study clearly showed that NPM was expressed scarcely in granulocytes, moderately in lymphocytes and erythroblasts and abundantly in myeloblasts, supporting the role of NPM1 in proliferation and differentiation. Because the amount of *NPM1* transcripts are decreased but still expressed in granulocytes, the NPM protein level may be controlled by a post-transcriptional manner. In MDS specimens, the staining pattern and intensity were almost similar to the normal BM. Accordingly, low expression levels in immunoblots might reflect the increased mature fractions in the BM cells. In conclusion, cytoplasmic localisation and/or significant reduction of NPM1 protein level rarely occur in MDS. The expression level of NPM1 should be further studied in the stem/progenitor cell fraction of MDS.

Acknowledgments

This study was supported by Grant-in-Aids from the National Institute of Biomedical Innovation (to T.N.), for Scientific Research (to T.N., T.U. and G.S.) and the Japan Leukemia Research Fund (to T.U.).

References

1. Korgaonkar C, Hagen J, Tompkins V, Frazier AA, Allamargot C, Quelle FW, et al. Nucleophosmin (B23) targets ARF to nucleoli and inhibits its function. Mol Cell Biol 2005;25:1258–1271.
2. Kurki S, Peltonen K, Latonen L, Kiviharju TM, Ojala PM, Meek D, et al. Nucleolar protein NPM interacts with HDM2 and protects tumor suppressor protein p53 from HDM2-mediated degradation. Cancer Cell 2004;5:465–475.

3. Colombo E, Marine JC, Danovi D, Falini B, Pelicci PG. Nucleophosmin regulates the stability and transcriptional activity of p53. Nat Cell Biol 2002;4:529–533.
4. Borer RA, Lehner CF, Eppenberger HM, Nigg EA. Major nucleolar proteins shuttle between nucleus and cytoplasm. Cell 1989;56:379–390.
5. Chan WY, Liu QR, Borjigin J, Busch H, Rennert OM, Tease LA, et al. Characterization of the cDNA encoding human nucleophosmin and studies of its role in normal and abnormal growth. Biochemistry 1989;28:1033–1039.
6. Falini B, Mecucci C, Tiacci E, Alcalay M, Rosati R, Pasqualucci L, et al. Cytoplasmic nucleophosmin in acute myelogenous leukemia with a normal karyotype. N Engl J Med 2005;352:254–266.
7. Grisendi S, Mecucci C, Falini B, Pandolfi PP. Nucleophosmin and cancer. Nat Rev Cancer 2006;6:493–505.
8. Naoe T, Suzuki T, Kiyoi H, Urano T. Nucleophosmin: a versatile molecule associated with hematological malignancies. Cancer Sci 2006;97:963–969.
9. Morris SW, Kirstein MN, Valentine MB, Dittmer K, Shapiro DN, Look AT, et al. Fusion of a kinase gene, ALK, to a nucleolar protein gene, NPM, in non-Hodgkin's lymphoma. Science 1995;267:316–317.
10. Yoneda-Kato N, Look AT, Kirstein MN, Valentine MB, Raimondi SC, Cohen KJ, et al. The t(3;5)(q25.1;q34) of myelodysplastic syndrome and acute myeloid leukemia produces a novel fusion gene, NPM-MLF1. Oncogene 1996;12:265–275.
11. Redner RL, Rush EA, Faas S, Rudert WA, Corey SJ. The t(5;17) variant of acute promyelocytic leukemia expresses a nucleophosmin-retinoic acid receptor fusion. Blood 1996;87:882–886.
12. Thiede C, Koch S, Creutzig E, Steudel C, Illmer T, Schaich M, et al. Prevalence and prognostic impact of NPM1 mutations in 1485 adult patients with acute myeloid leukemia (AML). Blood 2006;107:4011–4020.
13. Verhaak RG, Goudswaard CS, van Putten W, Bijl MA, Sanders MA, Hugens W, et al. Mutations in nucleophosmin (NPM1) in acute myeloid leukemia (AML): association with other gene abnormalities and previously established gene expression signatures and their favorable prognostic significance. Blood 2005;106:3747–3754.
14. Schnittger S, Schoch C, Kern W, Mecucci C, Tschulik C, Martelli MF, et al. Nucleophosmin gene mutations are predictors of favorable prognosis in acute myelogenous leukemia with a normal karyotype. Blood 2005;106:3733–3739.
15. Dohner K, Schlenk RF, Habdank M, Scholl C, Rucker FG, Corbacioglu A, et al. Mutant nucleophosmin (NPM1) predicts favorable prognosis in younger adults with acute myeloid leukemia and normal cytogenetics: interaction with other gene mutations. Blood 2005;106:3740–3746.
16. Suzuki T, Kiyoi H, Ozeki K, Tomita A, Yamaji S, Suzuki R, et al. Clinical characteristics and prognostic implications of NPM1 mutations in acute myeloid leukemia. Blood 2005;106:2854–2861.
17. Grisendi S, Bernardi R, Rossi M, Cheng K, Khandker L, Manova K, et al. Role of nucleophosmin in embryonic development and tumorigenesis. Nature 2005; 437:147–153.
18. Berger R, Busson M, Baranger L, Helias C, Lessard M, Dastugue N, et al. Loss of the NPM1 gene in myeloid disorders with chromosome 5 rearrangements. Leukemia 2006;20:319–321.
19. Oki Y, Jelinek J, Beran M, Verstovsek S, Kantarjian HM, Issa JP. Mutations and promoter methylation status of NPM1 in myeloproliferative disorders. Haematologica 2006;91:1147–1148.
20. Ozeki K, Kiyoi H, Hirose Y, Iwai M, Ninomiya M, Kodera Y, et al. Biologic and clinical significance of the FLT3 transcript level in acute myeloid leukemia. Blood 2004;103:1901–1908.
21. Xu JL, Lai R, Kinoshita T, Nakashima N, Nagasaka T. Proliferation, apoptosis, and intratumoral vascularity in multiple myeloma: correlation with the clinical stage and cytological grade. J Clin Pathol 2002;55:530–534.
22. Corey SJ, Minden MD, Barber DL, Kantarjian H, Wang JC, Schimmer AD. Myelodysplastic syndromes: the complexity of stem-cell diseases. Nat Rev Cancer 2007;7:118–129.
23. Sportoletti P, Grisendi S, Majid SM, Cheng K, Clohessy JG, Viale A, et al. Npm1 is a haploinsufficient suppressor of myeloid and lymphoid malignancies in the mouse. Blood 2008;111:3859–3862.

THE JOURNAL OF BIOLOGICAL CHEMISTRY VOL. 283, NO. 36, pp. 24420–24425, September 5, 2008

Acetylation of PML Is Involved in Histone Deacetylase Inhibitor-mediated Apoptosis*[S]

Received for publication, March 20, 2008, and in revised form, July 7, 2008 Published, JBC Papers in Press, July 11, 2008, DOI 10.1074/jbc.M802217200

Fumihiko Hayakawa[‡1], **Akihiro Abe**[‡], **Issay Kitabayashi**[§], **Pier Paolo Pandolfi**[¶], **and Tomoki Naoe**[‡]

From the [‡]*Department of Hematology and Oncology, Nagoya University, Graduate School of Medicine, Nagoya 466-8550, Japan, the* [§]*Molecular Oncology Division, National Cancer Center Research Institute, 5-1-1 Tsukiji, Chuo-ku, Tokyo 104-0045, Japan, and the* [¶]*Cancer Genetics Program, Beth Israel Deaconess Cancer Center, Department of Medicine, Harvard Medical School, Boston, Massachusetts 02215*

PML is a potent tumor suppressor and proapoptotic factor and is functionally regulated by post-translational modifications such as phosphorylation, sumoylation, and ubiquitination. Histone deacetylase (HDAC) inhibitors are a promising class of targeted anticancer agents and induce apoptosis in cancer cells by largely unknown mechanisms. We report here a novel post-transcriptional modification, acetylation, of PML. PML exists as an acetylated protein in HeLa cells, and its acetylation is enhanced by coexpression of p300 or treatment with a HDAC inhibitor, trichostatin A. Increased PML acetylation is associated with increased sumoylation of PML *in vitro* and *in vivo*. PML is involved in trichostatin A-induced apoptosis and PML with an acetylation-defective mutation shows an inability to mediate apoptosis, suggesting the importance of PML acetylation. Our work provides new insights into PML regulation by post-translational modification and new information about the therapeutic mechanism of HDAC inhibitors.

The promyelocytic leukemia protein PML controls cell cycle progression, senescence, and cell death (1, 2). Wild-type PML is a potent growth suppressor that, when overexpressed, can block cell cycle progression in a variety of tumor cell lines (1); conversely $PML^{-/-}$ mouse embryo fibroblasts (MEFs)[2] replicate significantly faster than their $PML^{+/+}$ MEFs (3). PML also plays an essential role in DNA damage or stress-induced apoptosis, and $PML^{-/-}$ cells are resistant to a variety of apoptotic signals (4). In normal cells, the PML protein is localized in, and essential for the biogenesis of, discrete subnuclear compartments designated as nuclear bodies (NBs) (5). In NBs, PML coaccumulates with more than 70 kinds of proteins that are involved in tumor suppression, apoptosis, regulation of gene expression, anti-viral response, and DNA repair. PML is thought to exert its function by regulating the function of binding partners as a core of NBs (6). Intriguingly, NBs are disrupted in human acute promyelocytic leukemia cells by PML-RARα, a oncogenic fusion protein of PML, and RAR-α, which is thought to be the mechanism of anti-apoptotic effect of PML-RARα (7–9).

It has been reported that NB formation requires PML to be conjugated to SUMO-1 (5, 10). SUMO-1 is an 11-kDa protein that is structurally homologous to ubiquitin (11). Sumoylation is thought to regulate the subcellular localization, stability, DNA binding, and/or transcriptional ability of its target proteins such as PML, Ran GTPase-activating protein (RanGAP)1, IκBα, and heat shock transcription factor 2 (11). Virtually As_2O_3, a chemotherapeutic agent clinically used in the treatment of acute promyelocytic leukemia cells, induces PML sumoylation. Increased PML sumoylation induced by As_2O_3 treatment leads to the restoration of NBs disrupted by PML-RARα and then is followed by apoptosis in acute promyelocytic leukemia cells, which results in prolonged remission of the disease (12–15). These findings underscore the importance of PML sumoylation and the integrity of NBs to tumor suppression.

Histone deacetylase (HDAC) inhibitors, a promising class of targeted anticancer agents, can block proliferation and induce cell death in a wide variety of transformed cells (16). HDAC inhibitors block the activity of class I and II HDACs and induce histone acetylation, which leads to the relaxation of chromatin structure, enhanced accessibility of transcription machinery to DNA, and increased gene transcription (17). HDAC inhibitors also induce acetylation of transcription factors, which alters their activities and the expression of their target genes (18). Recent studies demonstrated that p53 acetylation induced by a HDAC inhibitor leads to expression of proapoptotic proteins such as Bax, PIG3, and NOXA (19, 20). However, the mechanisms of p53-independent apoptosis by HDAC inhibitor remain largely unknown.

Here, we report PML acetylation as its novel post-transcriptional modification. PML acetylation is induced by trichostatin A (TSA), a HDAC inhibitor. This enhanced acetylation leads to increased PML sumoylation and may play a key role in TSA-induced apoptosis. This work provides new insights into the

* This work was supported by grants-in-aid from the Uehara Memorial Foundation, the National Institute of Biomedical Innovation, and the Ministry of Education, Culture, Sports, Science, and Technology of Japan. The costs of publication of this article were defrayed in part by the payment of page charges. This article must therefore be hereby marked "*advertisement*" in accordance with 18 U.S.C. Section 1734 solely to indicate this fact.

[S] The on-line version of this article (available at http://www.jbc.org) contains supplemental Fig. S1–S9 and supplemental data.

[1] To whom correspondence should be addressed: Dept. of Hematology and Oncology, Nagoya University, Graduate School of Medicine, 65 Tsurumai-cho, Showa-ku, Nagoya, 466-8550, Japan. Fax: 81-52-744-2161; E-mail: bun-hy@med.nagoya-u.ac.jp.

[2] The abbreviations used are: MEF, mouse embryo fibroblast; HDAC, histone deacetylase; TSA, trichostatin A; NB, nuclear body; RAR, retinoic acid receptor; SUMO, small ubiquitin-like modifier; HAT, histone acetyltransferase; GST, glutathione *S*-transferase; HA, hemagglutinin; GFP, green fluorescent protein.

functional regulation of PML and the therapeutic mechanisms of treatment with HDAC inhibitors.

EXPERIMENTAL PROCEDURES

Antibodies, Plasmids, and Cell Culture—The sources of antibodies and plasmids and the cell culture conditions are detailed in the supplemental data.

Transient Transfection, Immunoprecipitation, Immunoblotting, Immunofluorescence, and in Vitro and in Vivo Acetylation Assays—These were performed as described previously (21, 28) except transient transfections into PML$^{-/-}$ MEFs were performed by nucleofection using the Nucleofector system (Amaxa Biosystems) according to the manufacturer's instructions.

Antibody Array Assay and Detection and Quantification of Apoptosis—These are also detailed in the supplemental data.

In Vitro Sumoylation Assay—The *in vitro* sumoylation assay was performed essentially as described previously (21), except recombinant SUMO E1 ligase purchased from BIOMOL International was used instead of HeLa cell lysate.

Cell Sorting—Cell sorting was performed using BD FACSAria Cell Sorter (BD Biosciences) according to the manufacturer's instructions.

RESULTS

PML Exists as an Acetylated Protein in HeLa Cells Treated with Trichostatin A—HDAC inhibitors including TSA induce differentiation, growth arrest, and apoptosis of cancer cells. In addition to their effects on histones, HDAC inhibitors increase the acetylation level of several non-histone proteins, such as transcription factors, cytoskeletal proteins, and molecular chaperones, which are important for their effects on cancer cells (18). These observations prompted us to screen new acetylation targets of TSA with an antibody array assay combined with *in vivo* labeling of acetylated proteins with [^{14}C]acetate. Seven spots indicating possible targets of TSA-induced acetylation were detected (supplemental Fig. S1 and Fig. 1*A*). We focused on one of these targets, PML, a multifunctional protein that is involved in apoptosis, tumor suppression, and cell cycle regulation (2). We set out to confirm whether PML was acetylated *in vivo*. The same anti-PML antibody as used in the antibody array assay immunoprecipitated an ~79-kDa acetylated protein from lysates of TSA-treated HeLa cells (Fig. 1*B*), suggesting that PML existed as an acetylated protein in them. Of note, the antibody we used detected only a single band of PML, although PML has seven isoforms. The antibody was confirmed to be able to detect all PML isoforms, suggesting that this PML was the main one expressed in HeLa cells (supplemental Fig. S1).

PML Is Acetylated by p300 and GCN5 in Vitro—To test whether known histone acetyltransferases (HATs), p300 and GSN5, can acetylate PML, we performed an *in vitro* acetylation assay using GST-PML as a substrate. Both HATs acetylated PML *in vitro* (Fig. 2*A*), and we focused on the acetylation by p300 that occurred with higher efficiency. Use of a series of PML subdomains in the *in vitro* p300 acetylation assay indicated that PML would be acetylated on the C-terminal domain, amino acids 448–560 (supplemental Fig. S2). Inspection of the

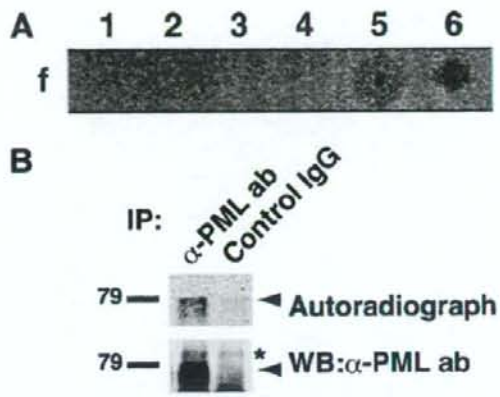

FIGURE 1. **PML exists as an acetylated protein in HeLa cells treated with TSA.** *A*, screening for acetylation targets of TSA by antibody array. Lysate from HeLa cells pulse-labeled with [^{14}C]acetate and treated with TSA was incubated with a nitrocellulose array comprising 113 antibodies. After extensive washes, the array was subjected to autoradiography. Similar results were obtained from duplicated experiments. Representative spots are shown. The antibodies used for *f-1* to *f-6* are anti-MEK1/2 antibody, anti-phospho-MEK1/2 antibody, anti-MKP-1 (V-15) antibody, anti-PML (PG-M) antibody, anti-PML (H-238) antibody, and anti-acetylated lysine antibody, respectively. *B*, PML exists as an acetylated protein in TSA-treated HeLa cells. Pulse-labeled HeLa cells with TSA treatment were lysed as in *A*. The lysates were immunoprecipitated (*IP*) with PML antibody (*ab*) or control rabbit IgG. 90% of the immunoprecipitates were subjected to SDS-PAGE, autoradiography, and detection with phosphorimaging (*upper panel*). 10% of the immunoprecipitates were subjected to SDS-PAGE and immunoblotting with PML antibody (*lower panel*). The positions of PML and nonspecific band are indicated by an *arrow* and an *asterisk*, respectively. *WB*, Western blotting.

PML sequence in this region revealed the presence of 7 lysine residues (supplemental Fig. S2); therefore, we introduced a series of arginine substitutions to map the acetylation sites. Within the C-terminal domain of PML, only the substitution of arginine for lysine 487 (K487R) measurably reduced acetylation of PML by p300 among all the individual substitutions (Fig. 2*B*; mutations are designated by the codon number between Lys and Arg). When arginine substitutions for other lysines were combined with K487R, a further reduction of acetylation was observed with K515R (Fig. 2*C*). Acetylation of full-length PML was impaired by substitutions of K487R and K487R/K515R similarly to that of the C-terminal domain of PML (Fig. 2*D*). Our results indicate that the principal sites of p300 acetylation in PML will be lysines 487 and 515.

PML Acetylation Is Increased in Response to TSA Treatment—We examined whether PML acetylation by p300 occurred *in vivo* at the same sites as identified *in vitro*. Wild-type PML and PML with the K487R/K515R mutations were designated as PML W and PML M, respectively. Coexpression of p300 enhanced PML W acetylation, whereas acetylation PML M was weak in the basal state and showed no significant response to p300 coexpression (Fig. 3*A*, *top panel*). The efficiency of immunoprecipitation was the same for all samples (Fig. 3*A*, *middle panel*), and the increase in acetylation of a 17-kDa protein by coexpression of p300, which suggested the induction of histone acetylation, was equal between transfectants with PML W and PML M (Fig. 3*A*, *bottom panel*). These results suggest that p300 acetylates PML *in vivo* at the same sites as identified *in vitro*.

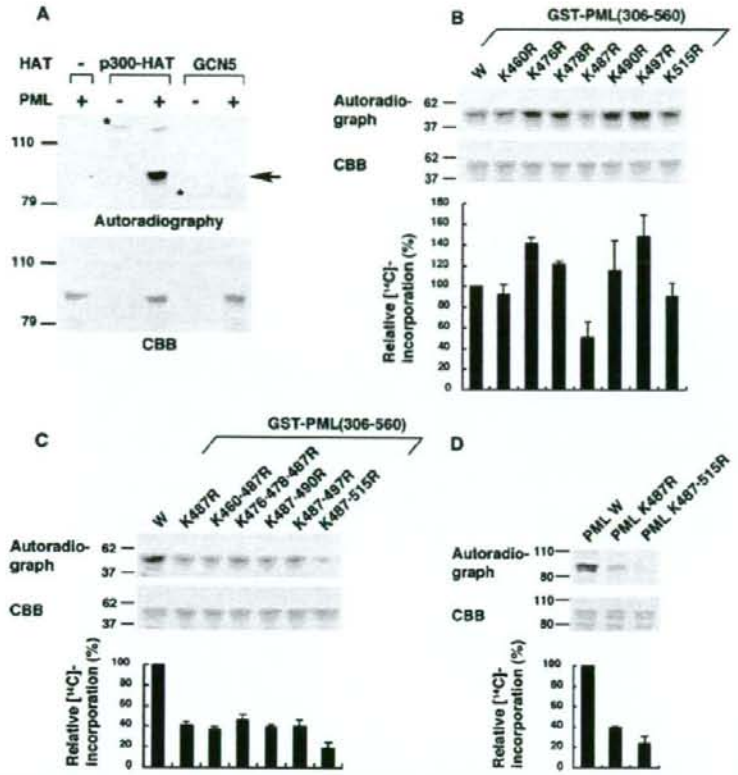

FIGURE 2. **PML acetylation *in vitro*.** *A*, PML is acetylated by p300 and GCN5. GST-PML was incubated with [^{14}C]acetyl-CoA and the indicated HATs. The reaction mixtures were subjected to SDS-PAGE, Coomassie Brilliant Blue (*CBB*) staining, and autoradiography. The positions of acetylated PML and acetylases are indicated by an *arrow* and *asterisks*, respectively. *B* and *C*, identification of PML acetylation sites. Wild-type or mutant GST-PML (amino acids 306–560) were subjected to *in vitro* acetylation by p300-HAT as in *A*. ^{14}C incorporation into each GST-PML construct was quantified using phosphorimaging. A representative phosphorimaging scan (*top panel*), the corresponding CBB-stained electrophoretogram (*middle panel*), and the quantitation of the ^{14}C incorporation for each mutant, relative to the wild-type PML construct (*bottom panel*), are presented. The averages of three independent analyses and standard deviations are shown. *D*, mutation of lysines in full-length PML reduced acetylation by p300. Wild-type or mutant GST-PML (full-length) were subjected to *in vitro* acetylation assays as described in *B*.

Next, we tested whether PML acetylation is induced by TSA. Similarly to the case of p300 coexpression, TSA treatment enhanced PML W acetylation, whereas acetylation of PML M was significantly reduced and showed no significant response to TSA treatment (Fig. 3*B*, *top panel*). Our results suggest that PML is an acetylation target of TSA and that PML acetylation in response to TSA largely occurs at the sites of acetylation by p300.

Acetylation of PML in Response to TSA Is Associated with Enhanced PML Sumoylation—Because one of the PML acetylation sites, lysine 487, is located in the putative nuclear localization signal (amino acids 476–490), we first examined whether PML acetylation affected its nuclear localization to see the effect of acetylation on PML function. However, TSA treatment and the acetylation-defective mutation did not obviously affect PML nuclear localization or accumulation to NBs in immunofluorescent staining (supplemental Fig. S3). We next investigated whether PML acetylation affected its sumoylation, which is required for PML to exercise many of its functions. We set up an *in vivo* sumoylation system in which conjugation of SUMO to PML could be detected by Western analysis, resulting in the appearance of a novel 100-kDa protein expected to be sumoylated PML (21). In this system, coexpression of p300 and exposure to TSA resulted in a significant increase in sumoylation of PML W, whereas sumoylation of PML M was weak and not obviously affected by these treatments (Fig. 4, *A* and *B*). These results suggest the possibility that PML acetylation at lysines 487 and 515 enhances its sumoylation. Next, to verify that acetylated PML is directly sumoylated, we set up an *in vitro* sumoylation system in which recombinant HA-tagged PML protein was incubated with recombinant SUMO E1 and E2 ligase and SUMO with or without a prior acetylation reaction using [^{14}C]acetyl-CoA. Autoradiography visualizing only acetylated PML demonstrated that acetylated PML was efficiently sumoylated (Fig. 4*C*, *upper panel*). Of note, sumoylation efficiency observed in the autoradiograph was much higher than that in immunoblotting with anti-HA antibody where acetylated and nonacetylated PML were visualized (Fig. 4*C*, *upper panel, lane 2 versus lower panel, lane 2*). These results indicate that acetylated PML may be preferentially sumoylated *in vitro*.

PML Acetylation May Play an Important Role in TSA-induced Apoptosis—TSA treatment induces apoptosis in HeLa cells by unknown mechanisms (16). In our previous study, PML sumoylation plays an important role in As_2O_3-induced apoptosis (21). Given our findings that PML acetylation is associated with increased PML sumoylation, this may represent one of the mechanisms of TSA-induced apoptosis. We first examined whether PML was involved in TSA-induced apoptosis. For this purpose, we established HeLa cells stably transfected with an expression vector for small hairpin RNA against PML and an empty control vector and designated them as PML KD HeLa and control KD HeLa, respectively. Successful knocking down of PML was confirmed by immunofluorescence analysis with an anti-PML antibody (supplemental Fig. S4). TSA treatment caused the appearance of a sub-G_1 peak in cell cycle analysis, a marker of apoptosis, in both cells. However, the ratio of apoptotic cells was reduced by ~60% in PML KD HeLa compared with control KD HeLa, suggesting the involvement of PML in

TSA-induced apoptosis (Fig. 5*A* and supplemental Fig. S5). We examined further using PML$^{-/-}$ MEFs. Notably, overexpression of PML W in PML$^{-/-}$ MEFs substantially increased TSA-induced apoptosis relative to cells transfected with an empty vector, whereas, PML M displayed an impaired ability to mediate apoptosis in response to TSA (Fig. 5*B* and supplemental Fig. S6). An equal expression level of PML between PML W and PML M transfectants was confirmed (supplemental Fig. S6). These results further support the involvement of PML in TSA-induced apoptosis and suggest the importance of PML acetylation in conferring apoptosis by TSA.

Next, we investigated the effect of PML sumoylation on PML-mediated apoptosis in response to TSA. Cotransfection of expression vectors for SUMO and Ubc9 further sensitized PML W transfectants to TSA-induced apoptosis (Fig. 5*C*, *third* and *fourth lanes*), whereas the proapoptotic effects of SUMO and Ubc9 were greatly reduced in control and PML M transfectants (Fig. 5*C*, *first* and *second lanes* and *fifth* and *sixth lanes*). Enhanced sumoylation of PML W induced by TSA and impaired sumoylation of PML M were observed also in PML$^{-/-}$ MEFs (Fig. 5*D*). These results suggest that sumoylation enhances PML-mediated apoptosis in response to TSA. To test this hypothesis, we created an expression vector for the PML-3K mutant, which had lysine-to-arginine mutations at all three PML sumoylation sites and cannot be sumoylated (22). Overexpression of PML-3K in either the presence or absence of SUMO and Ubc9 had little or no effect on TSA-induced apoptosis (Fig. 5*C*, *seventh* and *eighth lanes*), indicative of a requirement for PML sumoylation in TSA-mediated apoptosis. These results suggest the hypothesis that enhanced PML sumoylation through PML acetylation is one of the mechanisms of TSA-induced apoptosis.

Finally, to investigate the generality of the effects of TSA on PML among HDAC inhibitors, we used depsipeptide, another HDAC inhibitor that belongs to a different class. Depsipeptide enhanced acetylation and sumoylation of PML, and its apoptotic effect was increased by PML expression similarly to TSA (supplemental Fig. S8). These results further support the hypothetical importance of PML acetylation in HDAC inhibitor-induced apoptosis.

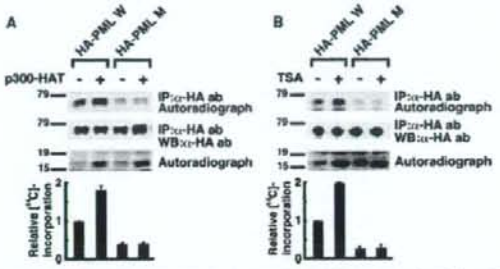

FIGURE 3. **PML acetylation *in vivo*.** *A*, PML acetylation is induced by p300 cotransfection *in vivo*. HeLa cells were transfected with indicated expression vectors. PML acetylation was analyzed as in Fig. 1*B* except for the use of anti-HA antibody (*ab*) instead of anti-PML antibody for IP and IB. The lysates were also subjected to SDS-PAGE followed by autoradiography to confirm successful induction of histone acetylation by p300-HAT cotransfection. A representative autoradiograph of PML (*top panel*), the corresponding image of IB with anti-HA antibody (*second panel from the top*), and the autoradiograph of histone (*third panel from the top*) are presented. ^{14}C incorporation into PML and the amount of immunoprecipitated (*IP*) PML protein were quantified using analyzer of each imaging system. Relative ^{14}C incorporation adjusted by the efficiency of immunoprecipitation was calculated. The average and standard deviations for two independent analyses are presented (*bottom panel*). *B*, PML acetylation is increased in response to TSA treatment. HeLa cells were transfected with indicated expression vectors and treated with or without 10 μM TSA for 4 h. PML acetylation was analyzed and presented as in *A*. *WB*, Western blotting.

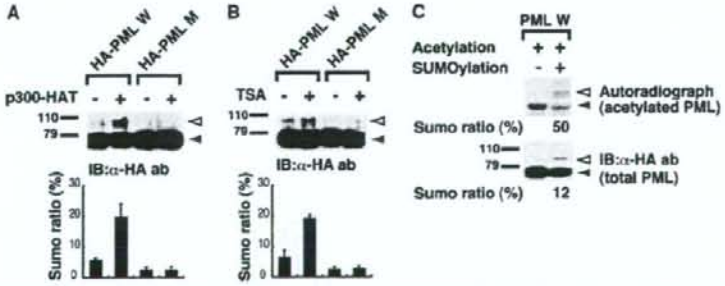

FIGURE 4. **PML acetylation is associated with enhanced sumoylation.** *A*, p300 coexpression enhances PML sumoylation. HeLa cells were transfected with the indicated expression vectors with cotransfection of those for SUMO and Ubc9. The cell lysates were subjected to SDS-PAGE followed by immunoblotting (*IB*) with anti-HA antibody (*ab*). The positions of sumoylated PML detected as an upper shifted band and nonsumoylated PML are indicated by *white* and *black arrowheads*, respectively. The ratios of sumoylated PML to total (sumoylated and unsumoylated PML) were calculated (SUMO ratio) and presented as bar charts. *B*, PML sumoylation increases in response to TSA treatment. PML sumoylation was examined as in *A* except that cells were treated with 10 μM TSA for 4 h instead of cotransfection of p300-HAT. *C*, acetylated PML is preferentially sumoylated *in vitro*. HA-tagged PML protein synthesized *in vitro* was immunoprecipitated with anti-HA antibody and incubated with p300-HAT and [^{14}C]acetyl-CoA as in Fig. 2*A*. The protein was subjected to an *in vitro* sumoylation assay and SDS-PAGE and transferred to a polyvinylidene difluoride membrane. Sumoylation of total (acetylated and nonacetylated) PML was visualized by IB with anti-HA antibody (*lower panel*). The same membrane was also subjected to an autoradiography to visualize sumoylation of acetylated PML (*upper panel*). Sumoylated and nonsumoylated PML are indicated as in *A*. SUMO ratio in each panel were calculated and presented at the *bottom*.

DISCUSSION

The data presented here demonstrate that acetylation of PML may enhance its sumoylation and play an important role in the control of PML-dependent apoptosis in response to TSA exposure. Sumoylation of PML is necessary for NB formation (5, 10), and the apoptotic effects of PML may be dependent on NB formation (see Introduction). Given our findings that PML acetylation is associated with increased PML sumoylation, this sumoylation-dependent NB formation may represent one of the mechanisms by which PML acetylation can enhance apoptosis. This hypothesis is supported by our findings that coexpression of SUMO and Ubc9 enhances PML-dependent apoptosis by TSA, that acetylation-defective mutants of PML exhibit defects in sumoylation and apoptosis in response to TSA treatment, and that a sumoylation-impaired PML mutant (PML-3K) is

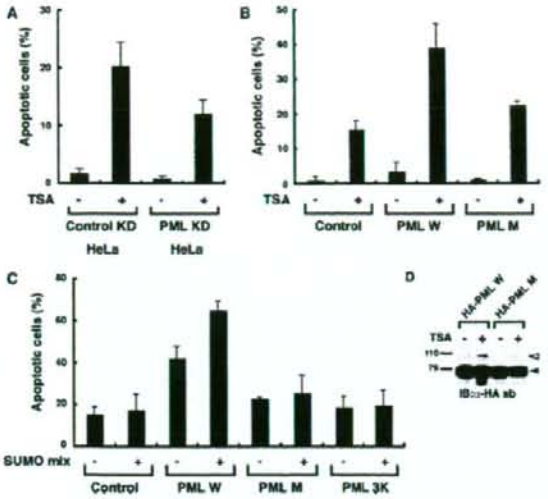

FIGURE 5. **PML acetylation is important for apoptosis induced by TSA.** *A*, PML knockdown reduces TSA-induced apoptosis in HeLa cells. HeLa cells whose PML was stably knocked down (PML KD HeLa) or control cells (Control KD HeLa) were treated with or without 1 μM TSA for 36 h. Apoptotic cells were detected and quantified as described under "Experimental Procedures." The ratios of apoptotic cells are plotted on bar charts. The averages of two independent analyses and standard deviations are shown. *B*, an acetylation-defective mutant of PML displayed impaired ability to mediate TSA-induced apoptosis. PML$^{-/-}$ MEFs were transfected with a bicistronic expression vector for GFP alone (control) or GFP and the indicated PML. GFP$^+$ cells were sorted and treated with or without 1 μM TSA for 48 h. Apoptotic cells were analyzed as in *A*. *C*, coexpression of Ubc9 and SUMO enhances PML-mediated apoptosis in response to TSA. The analyses of apoptosis were performed as in *B* except that cells were cotransfected with expression vectors for SUMO and Ubc9 (SUMO mix) or an empty vector as indicated. *D*, increased PML sumoylation induced by TSA in PML$^{-/-}$ MEFs. PML sumoylation in PML$^{-/-}$ MEFs was examined as in Fig. 4*B*. *IB*, immunoblotting; *ab*, antibody.

also defective in TSA-mediated apoptosis. It should be noted that PML$^{-/-}$ MEF cells are still sensitive to apoptosis by TSA, although at a much reduced level compared with cells expressing PML. There may also be PML-independent apoptotic mechanisms that respond to TSA. This is not surprising, considering that TSA alters the expressions of various genes by the acetylation of histones and many kinds of transcription factors such as p53 (see Introduction). More work will be required to determine the individual contributions of these different actions of TSA on the proliferation, survival, and differentiation of cells.

Acetylation of lysine leads to loss of its positive charge. In some cases, arginine, a positive charged amino acid, and glutamine, a noncharged one, are reported to mimic nonacetylated and acetylated lysine, respectively. We examined whether glutamine substitution at acetylation sites, lysines 487 and 515, had an enhancing effect on PML sumoylation. The PML mutant with glutamine substitution, however, showed impaired sumoylation in HeLa cells similarly to the one with arginine substitution (data not shown). Effects of acetylation other than the loss of positive charge or subtle differences of amino acid structure between lysine and glutamine may be important for PML sumoylation.

Recent studies reveal that increasing numbers of proteins are targeted by both acetylation and sumoylation. However, the correlation between these modifications has hardly been investigated except the cases where both modifications competitively target the same lysine residue such as the cases of HIC1 (hypermethylated in cancer 1) and MEF2 (myocyte enhancer factor 2) (23, 24). This is the first report that suggests acetylation-dependent enhancement of sumoylation. Phosphorylation has been reported to regulate sumoylation. Recently, the classical sumoylation consensus motif (ψKXE) with an adjacent proline-directed phosphorylation motif (SP), ψKXEXXSP motif where ψ is a large hydrophobic residue and X is any residue, has been proposed as a phosphorylation-dependent sumoylation motif (25, 26). Between the two acetylation sites, lysines 487 and 515, lysine 487 is the major acetylation site, and K487R affects sumoylation more than K515R (Fig. 2, *B* and *C*, and data not shown). PML sumoylation is reported to occur at three lysine residues, lysine 65, 160, and 490 (22). It would be interesting to discover whether acetylation at lysine 487 specifically affects sumoylation at any of these lysine residues, especially at the adjacent lysine 490. p53 also has a similar sequence where an acetylated lysine lies adjacent to a sumoylated lysine (supplemental Fig. S9), although the correlation between acetylation and sumoylation has not been investigated (27). K$\psi\psi$KXE might be a motif of acetylation-dependent sumoylation.

In summary, our studies provide evidence for a new post-transcriptional modification of PML and a new mechanism of regulation of PML sumoylation, and establish a novel relationship between PML and TSA-induced apoptosis. This work provides new insights into the regulation of PML function and the control of protein sumoylation. Considering the large number of binding partners of PML and the key contributions of PML to the stability and function of the NBs, PML acetylation is likely to modulate multiple cell activities beyond apoptosis through regulation of recruitment or release of NBs components.

Acknowledgments—We are very grateful to Ryouhei Tanizaki, Yuka Nomura, and Chika Wakamatsu for technical assistance.

REFERENCES

1. Mu, Z. M., Chin, K. V., Liu, J. H., Lozano, G., and Chang, K. S. (1994) *Mol. Cell. Biol.* **14,** 6858–6867
2. Salomoni, P., and Pandolfi, P. P. (2002) *Cell* **108,** 165–170
3. Wang, Z. G., Delva, L., Gaboli, M., Rivi, R., Giorgio, M., Cordon-Cardo, C., Grosveld, F., and Pandolfi, P. P. (1998) *Science* **279,** 1547–1551
4. Wang, Z. G., Ruggero, D., Ronchetti, S., Zhong, S., Gaboli, M., Rivi, R., and Pandolfi, P. P. (1998) *Nat. Genet.* **20,** 266–272
5. Ishov, A. M., Sotnikov, A. G., Negorev, D., Vladimirova, O. V., Neff, N., Kamitani, T., Yeh, E. T., Strauss, J. F., III, and Maul, G. G. (1999) *J. Cell Biol.* **147,** 221–234
6. Dellaire, G., and Bazett-Jones, D. P. (2004) *Bioessays* **26,** 963–977
7. Dyck, J. A., Maul, G. G., Miller, W. H., Jr., Chen, J. D., Kakizuka, A., and Evans, R. M. (1994) *Cell* **76,** 333–343
8. Koken, M. H., Puvion-Dutilleul, F., Guillemin, M. C., Viron, A., Linares-Cruz, G., Stuurman, N., de Jong, L., Szostecki, C., Calvo, F., Chomienne, C., Degos, L., Puvion, E., and de Thé, H. (1994) *EMBO J.* **13,** 1073–1083
9. Weis, K., Rambaud, S., Lavau, C., Jansen, J., Carvalho, T., Carmo-Fonseca, M., Lamond, A., and Dejean, A. (1994) *Cell* **76,** 345–356
10. Zhong, S., Muller, S., Ronchetti, S., Freemont, P. S., Dejean, A., and Pandolfi, P. P. (2000) *Blood* **95,** 2748–2752

11. Kim, K. I., Baek, S. H., and Chung, C. H. (2002) *J. Cell. Physiol.* **191,** 257–268
12. Muller, S., Matunis, M. J., and Dejean, A. (1998) *EMBO J.* **17,** 61–70
13. Zhu, J., Koken, M. H., Quignon, F., Chelbi-Alix, M. K., Degos, L., Wang, Z. Y., Chen, Z., and de The, H. (1997) *Proc. Natl. Acad. Sci. U. S. A.* **94,** 3978–3983
14. Chen, G. Q., Shi, X. G., Tang, W., Xiong, S. M., Zhu, J., Cai, X., Han, Z. G., Ni, J. H., Shi, G. Y., Jia, P. M., Liu, M. M., He, K. L., Niu, C., Ma, J., Zhang, P., Zhang, T. D., Paul, P., Naoe, T., Kitamura, K., Miller, W., Waxman, S., Wang, Z. Y., de The, H., Chen, S. J., and Chen, Z. (1997) *Blood* **89,** 3345–3353
15. Niu, C., Yan, H., Yu, T., Sun, H. P., Liu, J. X., Li, X. S., Wu, W., Zhang, F. Q., Chen, Y., Zhou, L., Li, J. M., Zeng, X. Y., Yang, R. R., Yuan, M. M., Ren, M. Y., Gu, F. Y., Cao, Q., Gu, B. W., Su, X. Y., Chen, G. Q., Xiong, S. M., Zhang, T., Waxman, S., Wang, Z. Y., Chen, S. J., Hu, J., Shen, Z. X., and Chen, S. J. (1999) *Blood* **94,** 3315–3324
16. Marks, P. A., Richon, V. M., and Rifkind, R. A. (2000) *J. Natl. Cancer Inst.* **92,** 1210–1216
17. Wolffe, A. P., and Pruss, D. (1996) *Cell* **84,** 817–819
18. Glozak, M. A., Sengupta, N., Zhang, X., and Seto, E. (2005) *Gene (Amst.)* **363,** 15–23
19. Bandyopadhyay, D., Mishra, A., and Medrano, E. E. (2004) *Cancer Res.* **64,** 7706–7710
20. Terui, T., Murakami, K., Takimoto, R., Takahashi, M., Takada, K., Murakami, T., Minami, S., Matsunaga, T., Takayama, T., Kato, J., and Niitsu, Y. (2003) *Cancer Res.* **63,** 8948–8954
21. Hayakawa, F., and Privalsky, M. L. (2004) *Cancer Cell* **5,** 389–401
22. Kamitani, T., Kito, K., Nguyen, H. P., Wada, H., Fukuda-Kamitani, T., and Yeh, E. T. (1998) *J. Biol. Chem.* **273,** 26675–26682
23. Stankovic-Valentin, N., Deltour, S., Seeler, J., Pinte, S., Vergoten, G., Guerardel, C., Dejean, A., and Leprince, D. (2007) *Mol. Cell. Biol.* **27,** 2661–2675
24. Gregoire, S., and Yang, X. J. (2005) *Mol. Cell. Biol.* **25,** 2273–2287
25. Hietakangas, V., Anckar, J., Blomster, H. A., Fujimoto, M., Palvimo, J. J., Nakai, A., and Sistonen, L. (2006) *Proc. Natl. Acad. Sci. U. S. A.* **103,** 45–50
26. Yang, X. J., and Gregoire, S. (2006) *Mol. Cell* **23,** 779–786
27. Kwek, S. S., Derry, J., Tyner, A. L., Shen, Z., and Gudkov, A. V. (2001) *Oncogene* **20,** 2587–2599
28. Hayakawa, F., Towatari, M., Ozawa, Y., Tomita, A., Privalsky, M. L., and Saito, H. (2004) *J. Leukocyte Biol.* **75,** 529–540

The Journal of Biological Chemistry ASBMB

bjh research paper

Clinical significance of nuclear non-phosphorylated beta-catenin in acute myeloid leukaemia and myelodysplastic syndrome

Jinglan Xu,[1] Momoko Suzuki,[1] Yousuke Niwa,[1] Junji Hiraga,[1] Tetsuro Nagasaka,[2] Masafumi Ito,[3] Shigeo Nakamura,[2] Akihiro Tomita,[1] Akihiro Abe,[1] Hitoshi Kiyoi,[4] Tomohiro Kinoshita[1] and Tomoki Naoe[1]

[1]Department of Haematology and Oncology, Nagoya University Graduate School of Medicine, Tsurumai-cho, Showa-ku, Nagoya, [2]Department of Clinical Pathophysiology, Nagoya University Graduate School of Medicine, Tsurumai-cho, Showa-ku, Nagoya, [3]Department of Pathology, Japanese Red Cross Nagoya 1st Hospital, Michishita-cho, Nakamura-ku, Nagoya, and [4]Department of Infectious Diseases, Nagoya University Hospital, Tsurumai-cho, Showa-ku, Nagoya, Japan

Received 5 June 2007; accepted for publication 11 September 2007

Correspondence: Jinglan Xu, Department of Haematology and Oncology, Nagoya University School of Medicine, 65 Tsurumai-cho, Showa-ku, Nagoya 466-8550, Japan. E-mail: xuj@med.nagoya-u.ac.jp

Summary

Wnt signaling activates the canonical pathway and induces the accumulation of non-phosphorylated beta-catenin (NPBC) in the nucleus. Although this pathway plays an important role in the maintenance of haematopoietic stem cells as well as in oncogenesis, the significance of nuclear NPBC remains unclear in malignant haematopoiesis. This study examined the expression of nuclear NPBC in bone marrow specimens from 54 and 44 patients with *de novo* acute myeloid leukaemia (AML) and myelodysplastic syndrome (MDS), respectively. On immunohistochemistry with an anti-NPBC antibody, the nuclei were positively stained in 22 and 18 of AML and MDS specimens, respectively. Staining of nuclear NPBC was associated with AML subtypes (M6 and M7), low complete remission (CR) rate, and poor prognosis. Nuclear NPBC was also associated with a high score when using the International Prognostic Scoring System (IPSS) for MDS and with −7/−7q and complex karyotypes. These findings suggest that *in situ* detection of nuclear NPBC by immunohistochemistry could provide new insights into the pathogenesis and prognosis of AML and MDS.

Keywords: beta-catenin, non-phosphorylated beta-catenin, acute myeloid leukaemia, myelodysplastic syndrome, immunohistochemistry.

The Wnt/beta-catenin pathway is involved in the self-renewal and proliferation of haematopoietic stem cells (Reya *et al*, 2003; Willert *et al*, 2003). Signaling is initiated by binding of Wnt proteins to transmembrane receptors of the Frizzeled family (Giles *et al*, 2003). In the absence of Wnt signals, a dedicated complex of proteins that includes the tumor suppressor gene product APC, axin, and glycogen synthase kinase-3-beta (GSK3-beta) phosphorylates specific serine and threonine residues within the N-terminal region of beta-catenin, which leads to the ubiquitination of beta-catenin and its degradation by proteasomes (Conacci-Sorrell *et al*, 2002; Noort *et al*, 2002; Staal *et al*, 2002; Giles *et al*, 2003). Wnt signals block GSK3beta activity, resulting in the accumulation of non-phosphorylated beta-catenin (NPBC), which is finally translocated to the nucleus (Noort *et al*, 2002; Staal *et al*, 2002). Nuclear NPBC interacts with T-cell transcription factor (TCF) and lymphoid enhancer factor (LEF), and it activates target genes such as *MYC* and *CCND1* (He *et al*, 1998; Tetsu & Maccormick, 1999). Therefore, nuclear NPBC is known to be oncogenic in many solid tumors (Bienz & Clevers, 2000; Polakis, 2000). Mutations of APC, beta-catenin, or axin, which are observed in various tumors, lead to stabilization of NPBC (Morin *et al*, 1997; Barker & Clevers, 2000).

In the bone marrow (BM), Wnt proteins activate the beta-catenin pathway and the non-obese severe combined immunodeficient (NOD-SCID)-repopulating capacity of normal haematopoietic stem cells. They lead to increased expression of *HOXB4* and *NOTCH1* implicated in the self-renewal of haematopoietic stem cells (Reya *et al*, 2003). Up-regulation of the beta-catenin pathway has been suggested in chronic myeloid leukaemia (CML)-derived granulocyte-macrophage progenitor cells (GMPs) and multiple myeloma (MM) cells (Derksen *et al*, 2004; Jamieson *et al*, 2004). Furthermore, beta-catenin reportedly plays a significant role in promoting cell proliferation, adhesion, and survival *in vitro* (Chung *et al*, 2002). The expression of beta-catenin is also enhanced by oncogenic FLT3 signals and associated with poor prognosis (Tickenbrock *et al*, 2005; Ysebaert *et al*, 2006). However, there are some contradictory reports. Studies of conditional knockout mice with a beta-catenin gene (*Ctnnb1*) deletion indicated that *Ctnnb1* is not indispensable for haematopoiesis (Cobas *et al*, 2004). Furthermore, an active form of *Ctnnb1* compromised haematopoietic stem cell maintenance and blocked differentiation in transgenic mice experiments (Simon *et al*, 2005). The role of the Wnt/beta-catenin pathway in malignant haematopoiesis therefore needs to be further elucidated.

According to previous studies, the expression of beta-catenin is associated with activation of the Wnt pathway as well as poor prognosis (Tickenbrock *et al*, 2005; Ysebaert *et al*, 2006). However, beta-catenin is associated not only with Wnt signaling but also with adherence junctions (Conacci-Sorrell *et al*, 2002). It is anchored to the cell inner surface membrane via cadherins. In normal bone marrow (BM), the vascular endothelium expresses a significantly higher amount of beta-catenin relative to the level in haematopoietic cells. Accordingly, immunohistochemical detection of nuclear NPBC would enable a better understanding of the role of beta-catenin in leukaemia.

This study investigated the subcellular localization of beta-catenin in BM specimens from acute myeloid leukaemia (AML) and myelodysplastic syndrome (MDS) patients using two anti-beta-catenin antibodies: one against C-terminal peptides and another against N-terminal non-phosphorylated peptides. The latter antibody detected nuclear NPBC, and positive staining for nuclear NPBC was associated with particular clinical characteristics of AML and MDS.

Table I. Clinical characteristics of AML and MDS patients according to nuclear NPBC expression.

	Nuclear NPBC$^+$	Nuclear NPBC$^-$	*P*-value
Patients with *de novo* AML	22	32	
Age (median)	54 (20–81)	53 (18–71)	NS
Sex/male/female	18/4	17/15	0·005
Laboratory data			
WBC ($\times10^9$/l; median)	3·5 (0·8–92·5)	5·3 (0·7–202·1)	NS
Hb (g/l; median)	74 (43–134)	98 (36–141)	0·01
PLT ($\times10^9$/l; median)	7·6 (0·3–170)	4·2 (1·1–27·3)	NS
PB blasts (%; median)	24 (0–82)	39 (0–99)	NS
BM blasts (%; median)	46·2 (20–86·5)	77·5 (29–98)	0·02
CR rate	13/22 (59·1%)	24/27 (88·9%)	0·01
Relapse rate	16/21 (76·2%)	14/24 (58·3%)	0·03
Patients with MDS	18	26	
Age	59 (26–76)	57 (22–89)	
Sex/male/female	12/6	16/10	0·05
Laboratory data			
WBC ($\times10^9$/l; median)	2·9 (1·2–9·0)	2·6 (1·6–5·9)	NS
Hb (g/l; median)	75 (46–151)	85 (47–127)	NS
PLT ($\times10^9$/l; median)	79 (7–122)	44 (7–400)	NS
BM blasts (%; median)	3 (0–30)	5 (0–30)	NS
IPSS score*			
Low risk	0	4	NS
Intermediate-1	4	12	NS
Intermediate-2	4	4	NS
High risk	3	1	0·04

NPBC, non-phosphorylated beta-catenin; AML, acute myeloid leukaemia; MDS, myelodysplastic syndrome; WBC, white blood cell count; Hb, hemoglobin concentration; PLT, platelet count; PB, peripheral blood; BM, bone marrow; CR, complete remission; IPSS, International Prognostic Scoring System.
*Full data was available in 32 of the 44 patients with MDS.

Materials and methods

Patient samples

For clinical samples, BM clots were obtained during routine diagnostic procedures. Beta-catenin expression was analyzed in BM specimens from patients newly diagnosed at the Nagoya University Hospital between 2000 and 2006 (Table I). The *de novo* AML patients consisted of 35 men and 19 women with a median age of 53 years (range, 20–81 years), and *FLT3* mutations were detected in seven of 22 patients with AML (31·8%). The MDS patients consisted of 28 men and 16 women with a median age of 57 years (range, 22–89 years). BM mononuclear cells were harvested by standard Ficoll/Paque density gradient centrifugation (Amersham Pharmacia Biosciences, Roozendaal, the Netherlands), and were suspended in RPMI 1640 medium supplemented with 10% fetal bovine serum, 100 IU/ml of penicillin G and 100 μg/ml of streptomycin.

Antibodies

For immunohistochemical and immunoblot studies, two monoclonal antibodies were used; one was against C-terminal peptides (clone14, IgG1; BD Transduction Laboratories/Life Science Research, Heidelberg, Germany), enabling recognition of pan beta-catenin (PBC), and the other was against

N-terminal-peptides (clone 8E4, IgG1; Alexis Biochemicals, Lausanne, Switzerland), enabling recognition of NPBC.

Immunohistochemical staining

Samples were fixed with ice-cold 4% paraformaldehyde for 16–24 h, embedded in paraffin, sectioned transversely (thickness, 3 μm), and processed for immunohistochemistry to determine the localization of beta-catenin. After removal of paraffin with xylene and dehydration with a series of ethanol solutions, the tissue sections were subjected to microwave irradiation (750 W) for 15 min in 0·01 mol/l citrate buffer (pH 6·0). The sections were then placed in an automated immunostainer (Ventana Medical Systems, Tucson, AZ, USA) as described (Xu *et al*, 2002). For negative controls, primary antibodies were replaced with mouse IgG. The subcellular distribution of beta-catenin (i.e. restriction to the nucleus or presence in the membrane) was assessed without knowledge of the French-America-British (FAB) subtypes, *FLT3* mutations or karyotypes. We investigated a single case twice for NPBC expression. The entire section was screened to find the region with the highest immunostaining. The score was determined in each case after counting at least 500 nuclei in 3–5 randomly selected regions. When 20% or more of the BM mononuclear cells were positive for nuclear staining of NPBC, they were classified as nuclear NPBC$^+$. The cut-off value of 20% was determined by the median distribution of the percentage of BM mononuclear cells stained by NPBC. As described in the results, some erythroblasts were positive for NPBC but the number was <20% except in the case of M6 patients. On the other hand, almost all blasts in M7 and other cases tested positive. The discrimination of cell types based on the 20% criterion therefore enabled a clear delineation.

Immunoblotting

Cell lysates from AML cells were extracted as previously described (Ozeki *et al*, 2004). A total of 1×10^6 cells were directly lysed in sample buffer and then subjected to sodium dodecyl sulphate-polyacrylamide gel electrophoresis on a 10% gel, and the separated proteins were transferred to a polyvinylidene difluoride membrane (Bio-Rad, Hercules, CA, USA). The membrane was initially incubated at room temperature for 1 h with 5% nonfat milk and 0·1% Tween-20 in Tris-buffered saline and then overnight with mouse monoclonal antibodies at a 1:2000 dilution in the same solution. After washing, the membrane was incubated for 1 h with a 1:5000 dilution of horseradish peroxidase-conjugated mouse antibodies to mouse IgG (MBL, Amersham, Bucks, UK), and immune complexes were then detected with enhanced chemiluminescence (ECL) reagents (Amersham).

Statistical analysis

The χ^2 test was used to calculate the difference of frequencies between nuclear NPBC$^+$ and NPBC$^-$ groups. The Mann–Whitney *U*-test was used to compare continuous variables. Kaplan–Meier curves were drawn using STATVIEW software (Macintosh; SAS Institute, Cary, NC, USA). *P*-values <0·05 were considered significant.

Results

Using an anti-beta-catenin C-terminal peptide antibody, beta-catenin was stained in the membrane and cytoplasm of erythroid cells from normal BM. In *de novo* AML specimens, significant staining was observed only in M6. This antibody also detected BM vessels whose density was increased in AML specimens as previously reported (Serinsöz *et al*, 2004; Fig 1A). On the other hand, an anti-N-terminal nonphosphorylated peptide antibody gave no significant staining in the normal BM. In AML specimens, nuclear NPBC was detected in erythroid blasts, megakaryoblasts and some myeloblasts (Fig 1A). In M6 specimens, nuclear NPBC was detected in 30–80% of myelomonocytic cells and nearly 100% of erythroblastic cells (Fig 1A). In M7 specimens, megakaryocytes were also strongly positive for nuclear NPBC (Fig 1A). In total, 20% or more of the BM mononuclear cells were positive for nuclear NPBC in 22 (40·7%) of 54 AML patients (Table I, Fig 1B). There was a strong male predominance of nuclear NPBC$^+$ cases, comprising 81·8% (18/22) in AML patients (Table I). However, the reason for this is unclear. In our cohort study, the karyotypes of female patients correlated to t(8;21)/t(15;17), which did not express nuclear NPBC. Thus the small numbers of studied patients seem to give some bias to the male predominance. A large-scale study is necessary to confirm this association. Nuclear NPBC$^+$ staining was closely associated with AML subtype: it occurred frequently (8/9) in M6 and M7 and rarely (0/7) in M3 (Fig 1B), and nuclear NPBC$^+$ was preferentially detected in erythroid and megakaryoblastic leukaemia compared to other myeloid leukaemias (M6–M7 vs. M0–M5, $P < 0·001$).

In MDS specimens, erythroid cells and endothelial cells were stained with the anti-beta-catenin C-terminal peptide antibody (Fig 2A). As observed for AML specimens, the cytoplasm and inner membrane were stained by this antibody. The anti-beta-catenin N-terminal nonphosphorylated peptide antibody detected nuclear staining in myeloblasts and erythroblasts that was similar to the pattern seen in AML cases (Fig 2A). Nuclear NPBC was found in 18 (40·9%) of 44 MDS patients, and was related to the FAB classification of MDS (Table I, Fig 2B). Nuclear NPBC$^+$ was preferentially detected in refractory anaemia with excess blasts in transformation (RAEBT) compared to other MDS subtypes [RAEBT *versus* refractory anaemia (RA)/refractory anaemia with ringed sideroblasts (RARS)/RAEB, $P = 0·01$].

To confirm whether these two antibodies recognized beta-catenin, a total of 41 samples from AML and MDS patients were subjected to immunoblot analysis. The anti-beta-catenin C-terminal peptide antibody detected bands at a molecular weight of 95 kDa, corresponding to beta-catenin, in most